Development of a Novel Software Tool for Co-optimisation of Energy, Reserve and Frequency Ancillary Services

Tool for Co-optimisation of Energy and Frequency-containment Services
Funding Source: NIA
Sponsor organisation: National Grid ESO

Imperial College Team

June 2024

Short summary

Imperial College Team has developed a novel software tool that can enable cost-effective selection of different frequency control services. (e.g., inertia, primary frequency response, dynamic containment, the reduced largest loss, etc.), through co-optimisation of energy, reserve and frequency regulation services. Frequency-security constraints have been integrated into the developed software tool, capturing Rate-of-Change-of-Frequency (RoCoF), frequency Nadir, frequency deviation in quasi-steady-state, etc., to meet the requirements for frequency control.

The developed software tool now explicitly links the technical and temporal characteristics of the different services, in order to operate the national electricity grid securely and cost-effectively. Furthermore, the novel software tool has been further enhanced to include reserve requirements, network constraints, synthetic inertia, demand-side inertia, etc., which will be implemented in the ESO control centre in the next phase. To give an overview of the developed software tool, this report specifically summarises the capabilities and key functions of the enhanced software tool and presents various case studies to verify the effectiveness of this software tool in achieving cost-effective co-optimisation of energy and frequency control services.

Contents

1. Background 5
2. Project Scope 6
3. Functions of the Software Tool 9
3.1. Tool Delivery 10
4. Problem Formulation 12
4.1. Frequency-related Constraints 12
4.2. UC Constraints 14
4.3. Reserve Constraints 15
4.4. Thermal Constraints 16
4.5. Synthetic Inertia modelling from Wind Turbines 17
4.6. Interconnector Constraints 17
4.7. Storage Constraints 17
4.8. Objective Functions 18
5. Case Studies 20
5.1. Co-optimisation of Energy and Frequency Services (COEF) 20
5.2. Co-optimisation for both Low and High Frequency Security 23
5.3. Co-optimisation of Energy and Reserve Requirement 24
5.4. Modelling Transmission Network Constraints 25
5.5. Influence of Adding Frequency-related Constraints 27
5.6. Synthetic Inertia and Demand-side Inertia 27
5.7. The Choice of 'Optimised Largest Loss' 30
5.8. Secure both Regions under Regional Frequency Model 32
6. Summary of the Testing and Results 33
6.1. Test Result Summary 33
6.1.1. Comparison between MATLAB and real-world frequency curves 33
6.1.2. Demonstration of Co-optimisation results 37

6.2. Sensitivity Analysis 39
7. Current Operational Practices in the Control Room....42
8. Needs and Requirements for the Evolution of the Prototype....43
9. Conclusions 44
References....45

1. Background

Decarbonisation of power systems introduces significant challenges, being one of the most significant deteriorations of frequency performance. This deterioration is mainly caused by the inertia reduction that comes associated with the integration of renewable energy resources (RESs), since RESs are decoupled from the power grid through power electronics converters and at present, do not naturally contribute to system inertia [1]. The reduced system inertia increases the required amount of frequency response to manage frequency security.

In order to maintain the electricity supply, frequency security must be assured, which means that the system's electric frequency should be contained within a narrow band around the nominal value of 50 Hz. In particular, the lack of system inertia exacerbates the need for fast frequency response services (e.g., inertia response, primary frequency response (PFR), and dynamic containment (DC), reduced largest loss, etc.) to maintain the frequency evolution within security boundaries and avoid, in the worst case, emergency demand disconnections.

To always maintain the system's frequency within these secure ranges, system operators schedule certain frequency services that would only come into play in the event of frequency deviation. Thus, the goal of the project is to develop a novel software tool that integrates mathematical models for achieving the co-optimisation of energy and frequency (COEF) control services (this has not yet been addressed internationally, which could place GB as a leader in delivering cost effective operation and control of future RES dominated electricity systems [2]). In order to operate the national electricity grid cost-effectively, the developed software tool explicitly links the technical and temporal characteristics of the different types of frequency services (e.g., PFR and DC) together with optimised largest loss.

2. Project Scope

The developed modelling tool can achieve the cost-effective co-optimisation of energy and frequency services, including inertia, fast and slow response, reduced largest loss, etc. To respect the current practice of GB system operation, frequency-related constraints have been incorporated into the enhanced software tool, which are briefly summarised as below [2][3]:

- ✓ **RoCoF Constraint**: Rate-of-Change-of-Frequency (RoCoF) should not exceed a certain limit in order to avoid the tripping of RoCoF-sensitive relays.
- ✓ **Nadir Constraint**: Frequency nadir (minimum/maximum value of frequency) must always be above a certain value to prevent the activation of Under-Frequency Load Shedding (UFLS).
- ✓ **Quasi-steady-state (q-s-s) Constraint**: Frequency drop must be arrested if the sum of frequency response is greater than the largest loss. Quasi steady state is defined as the stable value that frequency must reach 60 seconds after a power outage.
- ✓ **Minimum Inertia Constraint**: The minimum system inertia (encompassing all system-wide frequency response and inertia controls) should be maintained above a certain level, e.g., 140 GVA·s, depending on system operation requirements.

To maintain the system's frequency within these secure ranges at all times, system operators schedule certain frequency services that would only come into play in the event of a frequency deviation. Thus, the developed modelling tool has integrated mathematical models for achieving the co-optimisation of energy and frequency control services, which can place GB as a world leader in the operation and control of future RES dominated electricity systems. It is worth noting that this report is used for showcasing the modelling only (the actual figures are not linked directly with the GB system).

Specifically, with the emergence of new technologies in power grids, new possibilities arise for the delivery of frequency response. Some devices such as Battery Energy Storage Systems (BESS) have much faster dynamics than thermal generators, and therefore can deliver DC in a significantly shorter time. In the past, PFR was the only service considered to contain a frequency decline, for which response must be delivered within ten seconds after a generation-demand imbalance, while DC must be delivered in just one second. A graphical description of the FR services defined in GB is provided in Figure 2.1, along with an illustration of post-fault frequency regulation.

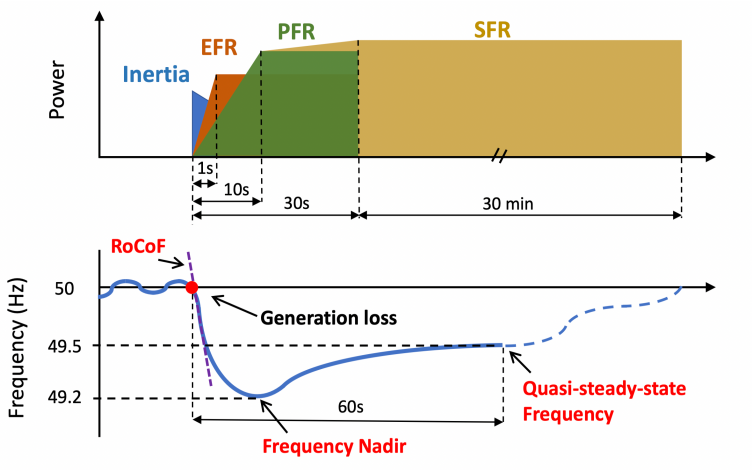

Figure 2.1: Post-fault frequency evolution and the limits that must be respected in GB as per National Grid regulation, along with the power contribution from the different frequency services defined: inertia, DC or EFR, PFR.

Furthermore, this non-uniform inertia distribution causes distinct regional frequencies as can be observed in Figure 2.2, obtained from the dynamic simulation of a two-region system where a generation outage occurs in Region 2.

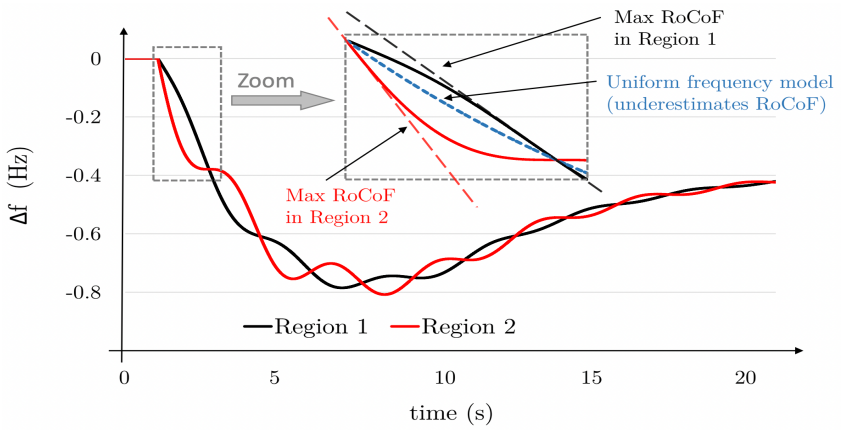

Figure 2.2: Frequency dynamics of two regions after a power outage in region 2

These geographical discrepancies in frequency have been observed after frequency events in recent years by utilities in number of countries [4]. From a frequency-security perspective, Figure 2.2 illustrates the dangers of considering the Centre of Inertia model in systems with non-uniform inertia distribution: frequency constraints deduced from the swing equation would underestimate the actual need for frequency services, leading to higher regional RoCoF and lower regional nadirs than expected (note that the frequency of the COI evolves in between the frequencies of the two areas, which exhibit some inter-area oscillations). If the scheduling optimisation is not appropriately constrained to reflect the distinct regional frequencies, unexpected tripping of RoCoF

relays and triggering of under frequency load shedding could take place, which in turn could cause cascading outages potentially leading to a blackout [4].

3. Functions of the Software Tool

The main goal of the developed software tool is to achieve the co-optimisation of energy and frequency services (COEF), while some other important functions are also included, such as network modelling, contingency modelling, reserve modelling, etc. Overall, the developed modelling tool is now equipped with the following key functions:

- ✓ **Time-Coupled Unit Commitment (UC) Model**: the developed software tool captures the detailed UC of each generator and determines the level of system inertia.
- ✓ **Dynamic-Frequency Requirements**: the constraints related to RoCoF, frequency Nadir, and quasi-steady-state requirements are deduced and integrated into the co-optimisation model.
- ✓ **Value of Inertia**: the co-optimisation modelling tool can quantity the value of inertia and include demand-side inertia.
- ✓ **Synthetic Inertia**: the scope of the software tool has been extended to consider the synthetic inertia from inverter-based resources, while the recovery effects of wind turbines are precisely modelled.
- ✓ **Co-optimisation of DC with Inertia and PFR**: the developed software tool is capable of achieving the co-optimisation of energy and different frequency services in order to minimise the overall operation costs.
- ✓ **Optimisation of Interconnector Power Flows to Reduce the Largest Loss**: the software tool can optimise the interconnection power imports and exports to minimise the total system operation costs while maintaining frequency stability.
- ✓ **Co-optimisation for both Under and Over Frequency Security**: the software tool includes the scheduling requirements for both under and over frequency constraints.
- ✓ **Reserve Modelling**: the software tool models provision of reserve from generators and storage units, which meets the system reserve requirement.
- ✓ **Transmission Network Constraints**: transmission network constraints are introduced in the co-optimisation model via DC optimal power flow, which can optimise the provision of energy and frequency regulation services, while managing transmission network congestions cost-effectively.

The key services, functions, and outputs of the co-optimisation software tool developed by Imperial College are illustrated in Figure 3.1. The developed model can achieve the co-optimisation of energy, frequency services, reserve requirements, and preventive control, obtaining cost-effective and secure scheduling results of generators, batteries, flexible demand, and interconnectors.

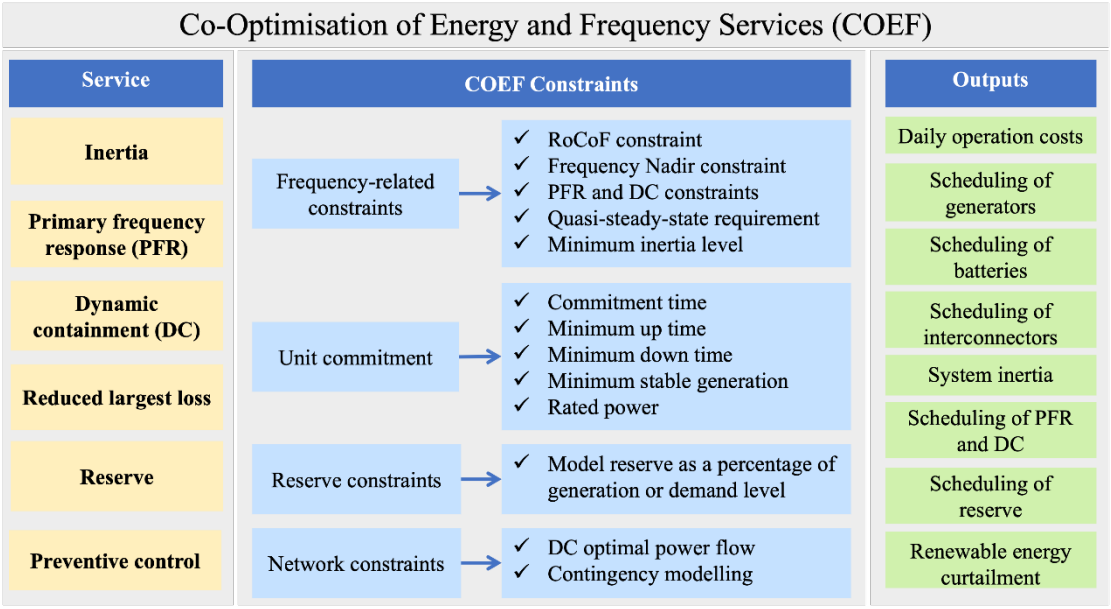

Figure 3.1: Illustration of the key services, functions, and outputs of the developed co-optimisation software tool

It is notable that the frequency services captured in the developed tool can be any type of ancillary services that enable compliment with frequency regulation requirements and support restoration of power equilibrium after a generation or demand outage. In current stage, frequency services involved in the enhanced co-optimisation software tool include:

- ✓ **Inertia** (either traditional inertia from synchronous generators or demand-side inertia as well as synthetic inertia from non-synchronous devices such as RES).
- ✓ **PFR** provided by conventional generators, such as gas-fired power plants.
- ✓ **DC** provided by appropriate technologies such as Battery Energy Storage Systems (BESSs).
- ✓ **Optimised largest loss** of generation or demand that can be influenced by the power imported and exported by interconnectors.

3.1. Tool Delivery

The uniform frequency model considers the concept of centre of inertia (COI), while the regional frequency model captures the spatial frequency differences between two regions (e.g., England and Scotland). Two different types of operation modes (e.g., centralised optimisation and 'self-dispatch') have been included. In summary, the developed co-optimisation tools are ready to be implemented.

Table 1 Summary of the delivered co-optimisation tool

	Uniform frequency model	**Regional frequency model**

Type 1	Centralised optimisation	Centralised optimisation
Type 2	Self-dispatch	Self-dispatch

4. Problem Formulation

Overall, the developed software tool incorporates frequency-related constraints, reserve constraints, and network constraints, achieving the co-optimisation of energy, frequency services and reserve requirements. The mathematical formulations of these key services provided in the co-optimisation model is presented in this section.

4.1. Frequency-related Constraints

The frequency-related constraints for under frequency security can be deduced from the swing equation, which describes the time evolution of frequency deviation after a generation outage [4]:

$$\frac{2H}{f_0} \cdot \frac{d\Delta f(t)}{dt} = \sum_{g \in G} PFR_g^{low}(t) + \sum_{s \in S} DC_s^{low}(t) - P_L^{low} \quad (1)$$

where H is the system inertia, P_L^{low} is the largest loss of generation, f_0 is the nominal frequency of the power grid, and $\Delta f(t)$ corresponds to the frequency deviation. $PFR_g^{low}(t)$ and $DC_s^{low}(t)$ indicate the PFR provided by generator g and the DC provided by battery s at time step t. In this context, the uniqueness of this tool, is the ability to include differential equation related to frequency variability in the mix-integer based system optimisation model, in order identify minimum operation costs, while meeting frequency stability constraints.

In this context, the system inertia can be calculated as:

$$H = \sum_{g \in G} H_g \cdot P_g^{max} \cdot N_g^{up} + H_D - H_L P_L^{low} \quad (2)$$

where H_g is the inertia constant of generating unit g, H_D is the demand-side inertia, P_g^{max} is the maximum power output of generating unit g, while N_g^{up} corresponds to the number of online generators of type g. To maintain the minimum inertia level (e.g., 140 GW·s), the following constraint is added into the co-optimisation model:

$$H \geq H_{min} \quad (3)$$

The constraint that guarantees RoCoF security is directly obtained from (1) by realising that the highest value for RoCoF is achieved at the very instant of the outage (t=0), when frequency deviation is effectively zero, i.e., $\Delta f(t) = 0$. Thus, the RoCoF constraint is expressed as:

$$|RoCoF| = \frac{P_L^{low} \cdot f_0}{2H} \leq RoCoF_{max} \quad (4)$$

where $RoCoF_{max}$ is the highest value allowed for RoCoF, e.g., 0.125 Hz/s. With the consideration of both PFR and DC, the frequency Nadir constraint can be expressed as:

$$|\Delta f_{nadir}| = |\Delta f_{t=t*}| \leq \Delta f_{max}^{low} \quad (5)$$

where t^* is the time when the nadir is reached. Δf_{max}^{low} corresponds to the maximum

allowable frequency deviation, e.g., 0.8 Hz. Let $t = t^*$, $\Delta f_{t=t*}$ can be written as:

$$\Delta f(\mathrm{t}^*) = \frac{\mathrm{f_0}}{2\mathrm{H}}\left[\frac{PFR_G^{low}}{2\mathrm{T_g}}(\mathrm{t}^*)^2 + DC_S^{low}\left(\mathrm{t}^* - \frac{\mathrm{T_s}}{2}\right) - P_L^{low}\cdot \mathrm{t}^*\right] \quad (6)$$

where $PFR_G^{low} = \sum_{g\in G} PFR_g^{low}$ and $DC_S^{low} = \sum_{s\in S} DC_s^{low}$. T_s and T_g are the service delivery time of DC and PFR, respectively. Note that the nadir must certainly occur before T_g, as otherwise frequency would drop indefinitely [4]. The time at which nadir is reached can be calculated by setting the derivative of frequency deviation in equation (1) to zero:

$$t^* = \frac{(P_L^{low} - DC_S^{low})\cdot T_g}{PFR_G^{low}} \quad (7)$$

By substituting (7) into (6), and then substituting the resulting expression into (5), the constraint that guarantees compliance with the nadir requirement can be expressed as [4]:

$$\left(\frac{H}{f_0} - \frac{DC_S^{low}\cdot T_s}{4\cdot\Delta f_{max}^{low}}\right)\cdot PFR_G^{low} \geq \frac{(P_L^{low} - DC_S^{low})^2\cdot T_g}{4\cdot\Delta f_{max}^{low}} \quad (8)$$

The constraint for assuring quasi-steady-state (q-s-s) security can be obtained from (1) by assuming that RoCoF is effectively zero in quasi-steady-state:

$$P_L^{low} - DC_S^{low} - PFR_G^{low} \leq 0 \quad (9)$$

Furthermore, the largest loss P_L can be modelled as a variable in the co-optimisation model rather than an input parameter, which is expressed as:

$$P_L^{low} \geq P_g(t),\ \forall\, g \in G \quad (10)$$

where the largest loss of generation can be caused by any large power source, e.g., the power importing behaviours of interconnectors or the power outputs of nuclear plants. Finally, by realising DM (dynamic moderation) and DR (dynamic regulation) as input parameters, the DC volume of storage *s* is limited by:

$$DM_s^{low} + DR_s^{low} + DC_s^{low} \leq \overline{\mathrm{P}}_s^{es} - \mathrm{P}_s^{esd} + \mathrm{P}_s^{esc},\ \forall\, s \in ES \quad (11)$$

where the binary variable u_s^{es} indicates the charging or discharging behaviours of ES *s* ($u_s^{es} = 1$, when the battery is charging). $\mathrm{P}_s^{esd}, \mathrm{P}_s^{esc}$ corresponds to the power discharging and charging of ES *s*, respectively.

Similarly, the largest loss of demand can be modelled in the similar manner, which might be caused by the disconnection of power exporting interconnector. Accordingly, the frequency-related constraints accounting for over frequency security are included:

$$|RoCoF| = \frac{P_L^{high}\cdot f_0}{2H} \leq RoCoF_{max} \quad (12)$$

$$\left(\frac{H}{f_0} - \frac{DC_S^{high}\cdot T_s}{4\cdot\Delta f_{max}}\right)\cdot PFR_G^{high} \geq \frac{(P_L^{high} - DC_S^{high})^2\cdot T_g}{4\cdot\Delta f_{max}^{high}} \quad (13)$$

$$P_L^{high} - DC_S^{high} - PFR_G^{high} \leq 0 \tag{14}$$

where the RoCoF constraint, frequency Nadir constraint, and q-s-s constraint are expressed in (12)-(14), respectively. In the case study carried out, over frequency security is supported by PFR_G^{high} and DC_S^{high} from generators and batteries, respectively. Δf_{max}^{high} corresponds to the maximum allowable frequency deviation, e.g., 0.5 Hz, for over frequency security.

4.2. UC Constraints

The developed UC model can capture the detailed operating characteristics of each individual generator, including their specific parameters: 1) rated power; 2) start-up time, MZT (Minimum Zero Time); 3) shut-down time, MNZT (Minimum Non-Zero Time); 4) ramp-up time and ramp-down time, RURE and RDRE (Ramp Up Rate Export and Ramp Down Rate Export; 5) minimum stable generation, SEL (Stable Export Limit); 6) maximum generation, MEL (Maximum Export Limit); 6) start generating time, NDZ (Notice to Deviate from Zero).

The scheduling behaviors of each individual generator can be modeled as:

$$y_{g,t} \cdot SEL_g \leq P_{g,t} \leq y_{g,t} \cdot MEL_g, \ \forall\, g \in G \tag{15}$$

$$P_{g,t} - P_{g,t-1} \leq y_{g,t} \cdot RURE_g, \quad \forall\, g \in G \tag{16}$$

$$P_{g,t-1} - P_{g,t} \leq y_{g,t} \cdot RDRE_g, \ \forall\, g \in G \tag{17}$$

$$y_{g,t} = y_{g,t-1} + \mathrm{y}_{g,t-1}^{sg} - \mathrm{y}_{g,t}^{sd}, \ \forall\, g \in G \tag{18}$$

$$\mathrm{y}_{g,t}^{sg} = \mathrm{y}_{g,t-\mathrm{T}_{g,t-NDZ_g}^{st}}^{st}, \forall\, g \in G \tag{19}$$

$$\mathrm{y}_{g,t}^{st} \leq \left(1 - y_{g,t-1}\right) - \textstyle\sum_{\tau=t-\mathrm{MNZT}_g}^{t} \mathrm{y}_{g,\tau}^{sd}, \forall\, g \in G \tag{20}$$

$$\mathrm{y}_{g,t}^{sd} \leq y_{g,t-1} - \textstyle\sum_{\tau=t-\mathrm{MZT}_g}^{t} \mathrm{y}_{g,\tau}^{sg}, \forall\, g \in G \tag{21}$$

where the generation and ramp-up/down limits of generators are modelled in (15)-(16). Constraint (18) represents the commitment state of a unit g is 'on' if it was generating in the previous time step or has started generating in the current time-step, unless it has been shut down in the current time-step. Constraint (19) means that the generator unit g starts generating if it was started up 'NDZ_g' hours before. Constraint (20) represents the generator that is allowed to start up if it was 'off' in the previous time-step and has been 'off' for at least 'MNZT_g' hours. Constraint (21) represents the unit that is allowed to be shut down if it was generating in the previous time-step, but also has been generating for at least 'MZT_g' hours. In detail, $y_{g,t}$ is a binary variable {0,1} corresponding to the commitment state of generator g at time step t. $\mathrm{y}_{g,t}^{sg}$ is the

binary variable that represents the 'start generating' state of generator g at time step t. $y_{g,t}^{sd}$ is the shut-down variable for generator g at time step t, while $y_{g,t}^{st}$ is the start-up variable for generator g at time step t [4]. The current co-optimisation model has half-hourly time resolution, so related UC parameters such as NDZ, MNZT, and MZT are expressed in 'half-an-hour' basis. If shorter timescale would be required for more accurate expressions of UC parameters, the time resolution of the co-optimisation model can be modified from 'half-an-hour' basis to 'minute' basis. For example, the time resolution can be reduced to '10 minutes' (or lower duration), where there will be there time slots in half-an-hour time scale.

The above formulation is used for the UC setup of generators, while the co-optimisation model can also include the UC setup of some 'load' units on demand side. In this context, demand related constraints can be added into the model including to 'SIL' (stable import limit) and 'MIL' (maximum import limit).

4.3. Reserve Constraints

The reserve can be provided by generators to meet demand-supply balance when there is sudden increase in demand, generation reduction, e.g., wind generation shortage. Operating reserve requirements can be determined by forecasting errors of wind output, PV output, electricity load and the capacity of the largest generator to cover the worst case [5]. In the enhanced software tool, the reserve requirement is modelled as a certain percentage of the demand level and realised as an input parameter. It is also notable that some other criterion (e.g., wind forecasting errors) can also be used, which depends on specific real-world situations. In detail, the 'low' reserve from each individual generator used to deal with 'lack of generation' is modelled as:

$$P_g(t) + \mathrm{PFR}_g^{low}(t) + \mathrm{RE}_g^{low}(t) \leq MEL_g(t), \ \forall\, g \ \in G \tag{22}$$

where $P_g(t)$ is the power output of generator g at time step *t*. $\mathrm{RE}_g^{low}(t)$ corresponds to the 'low' reserve provided by generator g at time step t, which is limited by the export power limit $MEL_g(t)$. Similarly, the 'high' reserve used to deal with 'demand loss' is modelled as:

$$P_g(t) - \mathrm{PFR}_g^{high}(t) - \mathrm{RE}_g^{high}(t) \leq SEL_g(t), \ \forall\, g \ \in G \tag{23}$$

where both 'low' and 'high' reserve of each individual generator at a certain time step t should be limited by a ramping rate.

The total 'low' reserve provided by all the generators should meet the following requirement:

$$\sum_{g \in G} \mathrm{RE}_g^{low}(t) \geq \alpha \cdot \mathrm{WT}_t \tag{24}$$

where WT_t is the wind generation level at time step t, while $\alpha \in [0,1]$ is realised as an input parameter to adjust the required reserve level. Normally, the value of α is around 3%-5%. Similarly, the total 'high' reserve can be modelled as a certain percentage of the demand level. Note that the selections of these criteria are just used

for showcasing purposes only. Other realistic criteria could also be used, following the current operating practice.

4.4. Thermal Constraints

The software tool has been extended to include the modelling of transmission network constraints via DC optimal power flow (OPF), which are expressed as:

$$\sum_{g\in G_i} P_g(t) - \mathrm{P}_i^d(t) = \sum_{ij\in L_i} P_{ij}(t),\ \forall\, i \in B \tag{25}$$

$$P_{ij}(t) = \frac{\theta_{ij}(t)}{x_{ij}}, \forall\, ij \in L \tag{26}$$

$$\theta_{ij}^{min} \le \theta_{ij}(t) \le \theta_{ij}^{max},\ , \forall\, i,j \in B \tag{27}$$

$$P_{ij}^{min} \le P_{ij}(t) \le P_{ij}^{max}, \forall\, ij \in L \tag{28}$$

$$\theta_i(t) = 0, if\ i = B^{ref} \tag{29}$$

where B and L correspond to the set of buses and lines in the transmission network, respectively. Constraints (25) and (26) refer to the nodal power balance respecting the Kirchhoff's current law (KCL). $\mathrm{P}_i^d(t)$ indicates the demand level of bus *i* at time step *t.* $P_{ij}(t)$ is the active power flow from network node *i* to node *j* at time step *t*, while x_{ij} is the reactance of transmission line *i-j*. $\theta_{ij}(t)$ corresponds to the voltage angle difference between bus *i* and bus *j*, which is limited by constraint (27). Finally, the power flow through line *i-j* is limited by constraint (28), while equation (29) indicates the voltage angle of the reference bus B^{ref} is set as 0.

Furthermore, the objective of the preventive control function is to prepare the system when it is still in normal operation, so that the system is able to face future uncertain events in a satisfactory way. The generator rescheduling is based on the outage of one transmission line linking two areas without violating line constraints. To this end, the software tool has been extended to take into account preventive control by modifying the network constraint (28) as:

$$e_{ij}(t,s) \cdot P_{ij}^{min} \le P_{ij}(t,s) \le e_{ij}(t,s) \cdot P_{ij}^{max}, \forall\, ij \in L, \forall\, s \in S \tag{30}$$

where the set S corresponds to various potential outage scenarios. In each outage scenario, there is one outage of the transmission line. In this context $e_{ij}(t,s)$ is used as input parameter, indicating the status of transmission line *i-j* under the scenario *s* (outage if $e_{ij}(t,s) = 0$).

In this context, the preventive control function of the software tool has been modelled by co-optimising all different outage scenarios. As a result, each individual generator *g* will schedule a certain amount of reserve $RE_g(t)$ to handle these potential line outages and ensure demand-supply balance under any outage situation, which can be expressed as:

$$P_g(t,s) \le P_g(t) + RE_g(t),\ \forall\, g\ \in G \tag{31}$$

where $P_g(t,s)$ is the rescheduled power output of generator g under outage scenario s.

4.5. Synthetic Inertia modelling from Wind Turbines

In the near future, RESs are expected to largely replace gas based synchronous generators in order to meet decarbonisation targets. In fact, inverter-based resources have the capability to contain frequency variations via synthetic inertia provision, if appropriately controlled. Synthetic inertia from wind generation is in essence a delivery of energy when it is most needed, but it needs appropriate power injection to compensate the recovery effect (such as PFR).

After considering synthetic inertia from wind turbines, the inertia equation (2) can be rewritten as:

$$H = \sum_{g\in G} H_g \cdot P_g^{max} \cdot N_g^{up} + H_D + \sum_{g\in WT} H_g^{wt} \cdot P_g^{wt} - H_L P_L^{low} \tag{32}$$

where H_g^{wt} is the inertia constant of wind turbine g. P_g^{wt} is the power output of wind turbine g. Additionally, due to the recovery effect of wind turbines, the q-s-s constraint for under frequency security should be rewritten as:

$$P_L^{low} + k_{rec} \cdot \sum_{g\in WT} H_g^{wt} \cdot P_g^{wt} - DC_S^{low} - PFR_G^{low} \le 0 \tag{33}$$

where the value of 'k_{rec}' is a design parameter for the wind turbine controller, since the recovery will be higher if the turbine provides synthetic inertia for a longer period, and lower otherwise [12].

4.6. Interconnector Constraints

The developed co-optimisation model is capable of scheduling interconnectors based on the provided power exporting (negative) and importing (positive) limits, which can be expressed as:

$$\mathrm{IC}_{i,t}^{min} \le \mathrm{P}_{i,t}^{ic} \le \mathrm{IC}_{i,t}^{max},\ \forall\, g \in IC \tag{34}$$

where $\mathrm{P}_{i,t}^{ic}$ is the power output of interconnector i at time step t. $\mathrm{IC}_{i,t}^{min}$ and $\mathrm{IC}_{i,t}^{max}$ correspond to the power exporting and importing limits of interconnector i at time step t, respectively.

4.7. Storage Constraints

The operation model of storage s is formulated as

$$0 \le P_{s,t}^{esc} \le u_{s,t}^{es} \cdot \bar{P}_s^{es}, \forall s \in S, \forall t \in T \tag{35}$$

$$-(1 - u_{s,t}^{es}) \cdot \bar{P}_s^{es} \le P_{s,t}^{esd} \le 0, \forall s \in S, \forall t \in T \tag{36}$$

$$\underline{S}_s^{es} \le S_{s,t}^{es} \le \bar{S}_s^{es}, \forall s \in S, \forall t \in T \tag{37}$$

$$S_{s,t+1}^{es} = S_{s,t}^{es} + \frac{P_{s,t}^{esc}\Delta t\eta_s^{esc} + P_{s,t}^{esd}\Delta t/\eta_s^{esd}}{\bar{E}_s^{es}}, \forall s \in S, \forall t \in T \quad (38)$$

where constraints (35) and (36) restrict charging and discharging power limits of storage s at time step t; the binary variable $u_{s,t}^{es} \in \{0,1\}$ indicates its charging ($u_{s,t}^{es} = 1$) or discharging ($u_{s,t}^{es} = 0$) status. Constraint (37) limits the minimum and maximum battery state-of-charge (SoC) level of storage s, while its dynamic transition between two consecutive time steps is presented in (38), given charging/discharging power as well as charging/discharging coefficients $\eta_s^{esc}/\eta_s^{esd}$.

4.8. Objective Functions

4.8.1 Centralised dispatch

The objective function this software tool is defined as the minimization of daily operation costs, which can be written as:

$$\begin{aligned}\min F^{central} = &\sum_{t\in T}\sum_{g\in G} P_g(t)\,\mathrm{c}_g^{gen}(t) + \sum_{t\in T}\sum_{g\in G} RE_g(t)\,\mathrm{c}_g^{re} \\ &+ \sum_{t\in T}\sum_{g\in G} PFR_g(t)\,\mathrm{c}_g^{PFR}(t) + \sum_{t\in T}\sum_{s\in S} DC_s(t)\,\mathrm{c}_s^{DC}(t) \\ &+ \sum_{t\in T}\sum_{i\in IC} \mathrm{P}_i^{ic}(t)\,\mathrm{c}_i^{ic}(t)\end{aligned} \quad (39)$$

where *IC* indicates the set of interconnectors in the power system. $\mathrm{c}_g^{gen}(t)$ and c_g^{re} are the generation cost and reserve cost of generator *g*, while $\mathrm{c}_g^{PFR}(t)$ and $\mathrm{c}_s^{DC}(t)$ are the PFR procurement cost of generator g and the DC procurement cost of battery *s*, respectively. $\mathrm{c}_i^{ic}(t)$ is the power importing cost or exporting revenue of interconnector i. This objective function includes generation costs, reserve costs, frequency service procurement costs, and interconnector costs towards the cost-effective co-optimisation of energy, frequency services, and reserve. Furthermore, it is worth noting that this objective function that is currently used, could be modified or expanded if further functions would be required.

4.8.2 Self-dispatch

Specifically, to respect the current market operation practices, the objective function can also be modified for self-dispatch purposes, which is expressed as:

$$\begin{aligned}\min F^{self} = &\sum_{t\in T}\sum_{g\in G} (\mathrm{P}_g^{buy}(t)\,\mathrm{c}_g^{offer}(t) - \mathrm{P}_g^{sell}(t)\,\mathrm{c}_g^{bid}(t)) \\ &+ \sum_{t\in T}\sum_{g\in G} RE_g(t)\,\mathrm{c}_g^{re} + \sum_{t\in T}\sum_{g\in G} PFR_g(t)\,\mathrm{c}_g^{PFR}(t) \\ &+ \sum_{t\in T}\sum_{s\in S} DC_s(t)\,\mathrm{c}_s^{DC}(t) \\ &+ \sum_{t\in T}\sum_{i\in IC} (\mathrm{P}_i^{ic,buy}(t)\,\mathrm{c}_i^{ic,offer}(t) - \mathrm{P}_i^{ic,sell}(t)\,\mathrm{c}_i^{ic,bid}(t))\end{aligned} \quad (40)$$

where $\mathrm{P}_g^{buy}(t)$ and $\mathrm{P}_g^{sell}(t)$ correspond to the energy bought from the market or sold back to the market at time step t, respectively in order to maintain demand-supply

balance. $c_g^{bid}(t)$ and $c_g^{offer}(t)$ are related to the energy bidding at time step t. Similarly, $P_i^{ic,buy}(t)$ and $P_i^{ic,sell}(t)$ correspond to the self-dispatching of IC i, while $c_i^{ic,bid}(t)$ and $c_i^{ic,offer}(t)$ are related to the energy bidding price and offering price of IC i. In this context, the main goal of the co-optimisation model is to minimise the re-dispatching costs of all the generators and interconnectors, while meeting energy and frequency stability requirements.

Additionally, the following constraints can be added into the co-optimisation model:

$$P_g(t) = P_g^{pn}(t) + P_g^{buy}(t) - P_g^{sell}(t),\ \forall g \in G, \forall t \in T \tag{41}$$

$$P_g^{buy}(t) \leq (1 - A_g(t)) \cdot M,\ \forall g \in G, \forall t \in T \tag{42}$$

$$P_g^{sell}(t) \leq A_g(t) \cdot M,\ \forall g \in G, \forall t \in T \tag{43}$$

where $P_g^{pn}(t)$ is the physical notification (PN) of generator g at time step t. $A_g(t)$ is a binary variable in $\{0,1\}$ to ensure $P_g^{buy}(t)$ and $P_g^{sell}(t)$ cannot occur simultaneously at time step t, where M is a very big number (e.g., 1000) corresponding to the 'big-M method'. The self-dispatching behaviours of ICs can be formulated in the same manner.

5. Case Studies

In order to clearly demonstrate the superior performance of the enhanced software tool in achieving the co-optimisation of energy and frequency services, extensive case studies have been carried out to analyse the key functions and capabilities discussed above, which are presented and discussed below. Specifically, the modelling tool developed by Imperial College Team, that is used for the scheduling of the power system generation, is called Unit Commitment (UC). The UC is a problem of particular interest when studying the provision of frequency services, since the scheduling of thermal generation determines the level of system inertia, the key driver of post-fault frequency evolution. In order to respect the current dispatching practice, the scheduling horizon of the developed co-optimisation model is set at 24 hours with half-an-hour resolution, i.e., 48-time steps.

5.1. Co-optimisation of Energy and Frequency Services (COEF)

The key focus of this COEF software tool is to achieve the co-optimisation of energy and various frequency services (e.g., inertia, PFR, DC and the reduced largest loss) from generators, energy storage devices and any other resources, while achieving minimum system operation costs.

In this context, the developed software tool is capable of co-optimising the operation of a large number of generators (around 600 generators), interconnectors and batteries, considering their complex and individual parameters, while minimising the total system costs, through the optimisation of the interaction between energy supply and frequency regulation services [4].

Specifically, DC is defined as a service for which response must be delivered in less than one second, as opposed to ten seconds for PFR. This service allows to recognise the faster dynamics in power injection of some novel technologies such as BESSs. The updated software tool can achieve the co-optimisation of energy and various frequency services, including DC, PFR, and inertia, etc. Specifically, to clearly present the key co-optimisation function, the developed model is solved using the data presented in the previous section, while the daily dispatches of various frequency response services are illustrated in Figure 5.1.

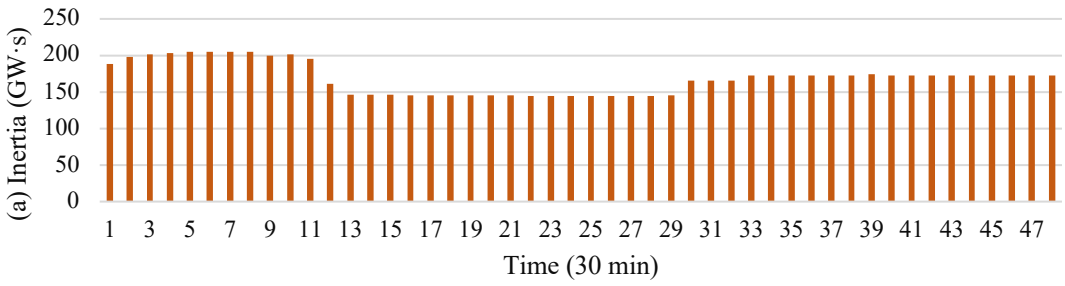

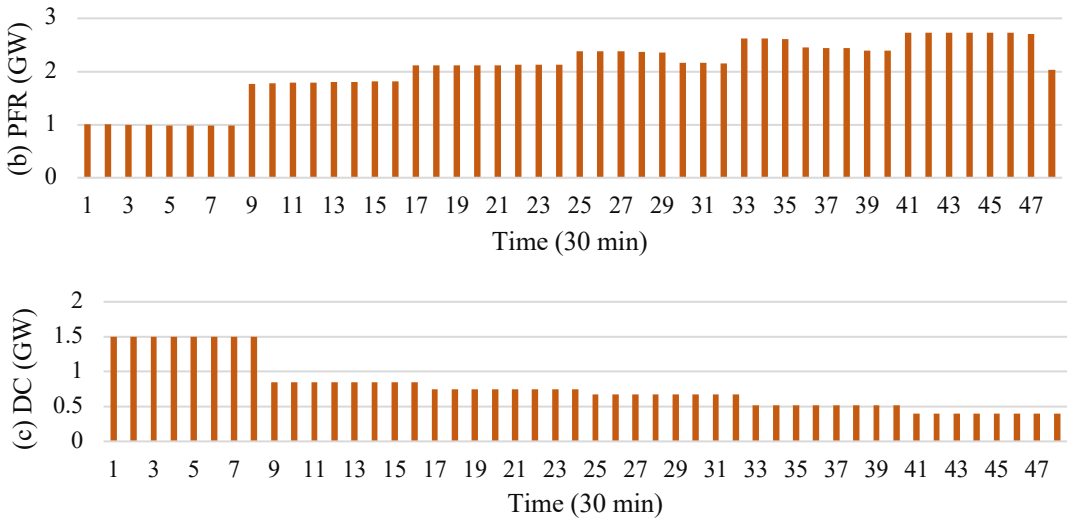

Figure 5.1: Scheduled frequency response services after solving the co-optimisation model: a) inertia, (b) PFR, and (c) DC

It can be observed from Figure 5.1(a) that the inertia level is maintained above 140 GW·s during the daily scheduling horizon, respecting the minimum inertia requirement. Note that this limit can also be changed as an input parameter according to current operating practices of GB power system. Figure 5.1(b) demonstrates that the DC schedules are maintained unchanged for every 8-time steps (4 hours), highlighting the Electricity Forward Agreement (EFA) block requirements [6].

Furthermore, in current frequency control framework, three types of dynamic frequency services, including Dynamic Containment (DC), Dynamic Moderation (DM) and Dynamic Regulation (DR), are considered in the new suite of Dynamic Response Services [6]. These services are used to control system frequency and keep it within the licence obligations of 50 Hz plus or minus 1%. Specifically, DM provides fast acting pre-fault delivery for particularly volatile periods, and DR is the staple slower pre-fault service, while DC is the post-fault service [7]. In the developed co-optimisation tool, the procurements of DM and DR from batteries are realised as input parameters, which will influence procurement of DC, as depicted in Figure 5.2. Obviously, due to the procurement of DM and DR, the quantity of DC procurement might be reduced. It is also notable that case studies conducted here only represent the co-optimisation results of one selected operating day to demonstrate the effectiveness of the developed software tool in achieving cost-effective co-optimisation of energy and frequency services. If the input data profiles change, the dispatch results of frequency services may change significantly.

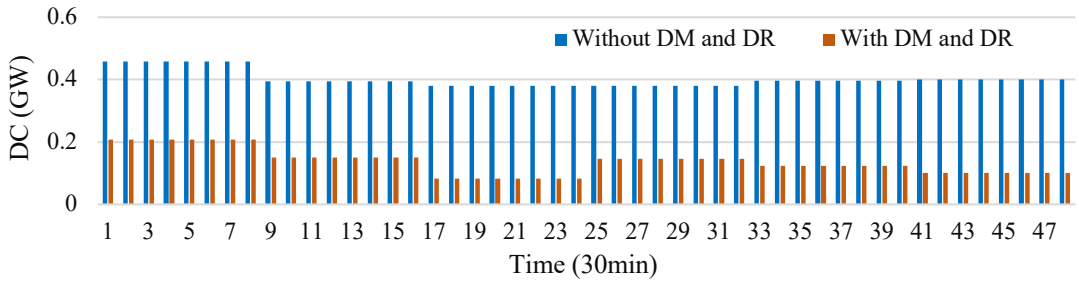

Figure 5.2: Impact of DM and DR services on the DC procurement

Finally, the developed software tool is capable of analysing the benefits of new frequency services through quantifying operation cost reduction. For example, due to the large-scale integration of electric vehicles (EVs) in future GB power system, cost-effective frequency services (e.g., DC) might be provided by EVs via vehicle-to-grid (V2G) technologies [8]. In this context, the enhanced software tool is capable of assessing the role and value of EVs in providing frequency regulation services. As illustrated in Figure 5.3, the co-optimisation tool reveals that large volumes of low-cost DC can reduce both the annual system operation cost and the annual cost of frequency regulation services very significantly.

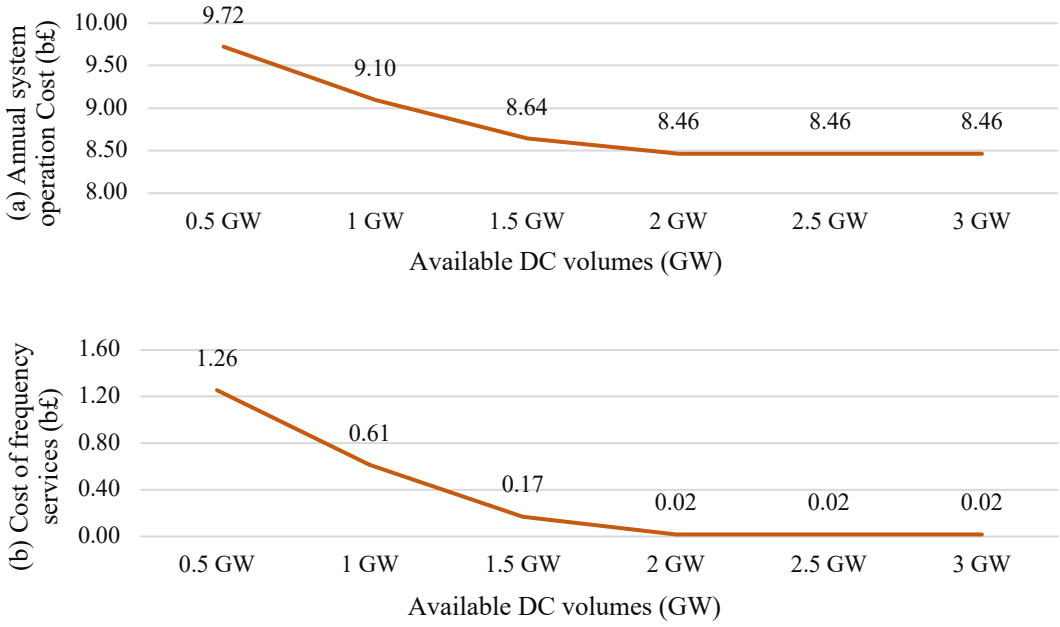

Figure 5.3: Annual system operation cost and annual cost of frequency services under different levels of low-cost DC

To this end, the enhanced software tool can achieve the co-optimisation of energy and various frequency services, including DC, DR, DM, PFR, and inertia, while it can also assist operators in analysing the benefits of new types of frequency regulation services, through quantifying the reduction in system operation costs as well as frequency service

procurement costs.

5.2. Co-optimisation for both Low and High Frequency Security

The scope of the COEF software tool is extended to include the scheduling requirements for both low and high frequency constraints. Specifically, in addition to low frequency security discussed in previous sections, the enhanced software tool can now consider the influence of the largest loss of demand (demand outage) on co-optimisation results through the incorporation of high frequency-related constraints, e.g., inertia, frequency Nadir (lower than 50.5 Hz), and rate-of-change-of-frequency (RoCoF) (lower than 0.125 Hz/s). In this context, generators and batteries are used to provide PFR and DC for both low and high frequency security requirements, respectively.

To accurately mimic low and high frequency security requirements, the power imports and exports by interconnectors have been included in the enhanced software tool, which can influence the largest loss of generation and demand. In detail, the power importing behaviours of interconnectors can influence the largest loss of generation accounting for under-frequency issues, while power exports via interconnectors can influence the largest loss of demand accounting for over-frequency issues. One example case study has been provided below to illustrate this. In detail, the largest losses of generation and demand for each time step are illustrated in Figure 5.4(a). The power importing and exporting behaviours of interconnectors are demonstrated in Figure 5.4(b), while the procurement of DC for both under and over frequency issues ('DC_low' and 'DC_high') is depicted in Figure 5.4(c).

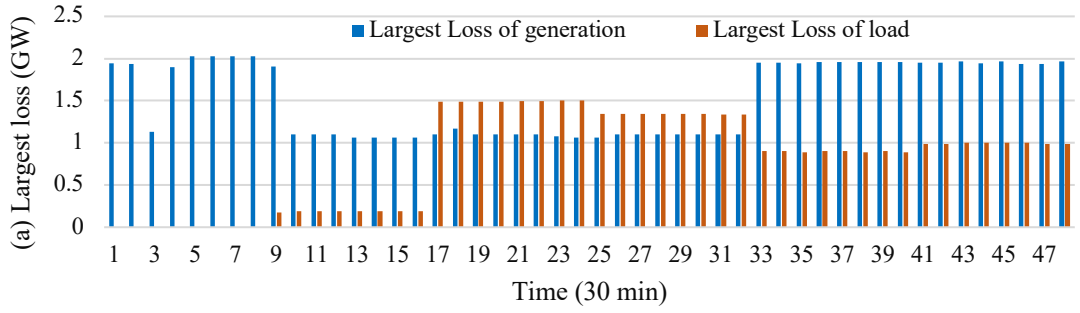

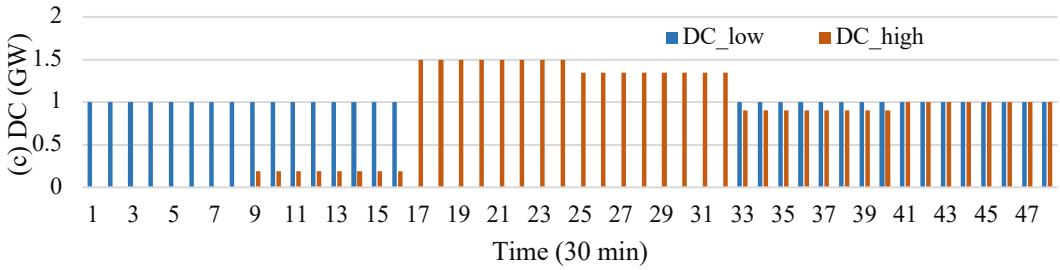

Figure 5.4: Co-optimisation results for the selected operating day: a) the largest loss of generation and demand, (b) power imports/exports of interconnectors, and (c) DC procurement for both over and under frequency response, i.e., 'DC_high' and 'DC_low'

It can be observed from Figure 5.4 (a) and (b) that the largest loss of generation may occur when some interconnectors (e.g., IFA) are importing power into the GB power system, while the largest loss of demand may occur when there are interconnectors (e.g., ElecLink) exporting power into other regions during time periods with high renewable generation production (e.g., time steps 17-33). In response to this, both low-frequency DC ('DC_low') and high-frequency DC ('DC_high') have been procured for frequency security, as presented in Figure 5.4 (c). Note that the case study presented considers one specific day, while the results could be significantly different under different system condition. Additionally, the updated software tool links the largest loss of demand driven by interconnectors that export power, while some other types of demand outages can also be easily incorporated into the COEF model.

5.3. Co-optimisation of Energy and Reserve Requirement

The software tool has been extended to include the co-optimisation of energy, reserve requirements, and frequency response services. There are two types of services procured from generators, including operating reserve and primary frequency response (PFR). Specifically, Reserve is a service that provides additional active power from generation or demand reduction. At certain times of the day, it may be necessary to access sources of extra power to manage actual demand on the system being greater than forecasted or unforeseen changes in generation availability [8]. When it is economic to do so, sources of extra power can be procured ahead of time through the reserve service. Providers of the service enable meeting the reserve requirement either by providing additional generation or demand reduction [9].

In the current COEF tool, the required reserve is assumed as a certain percentage of the demand level, while it is notable that some other criteria could also be used, depending on real-world requirements [10]. In this context, the delivery of reserve is coordinated by energy production and the provision of frequency regulation services towards the minimisation of daily operating costs. One example case study of co-optimisation of energy, reserve, and frequency response has been conducted, where the scheduling results of reserve and PFR from conventional generators are illustrated in Figure 5.5.

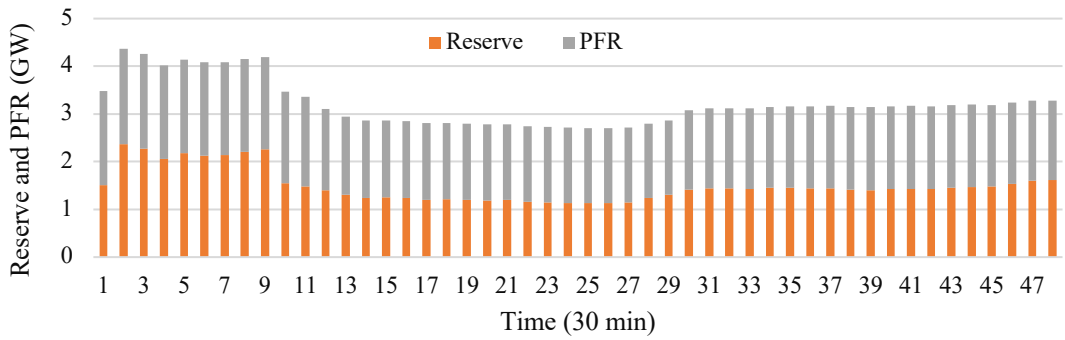

Figure 5.5: Illustration of reserve and PFR schedules in the co-optimisation of energy and balancing services

It can be observed from Figure 5.5 that there are two types of services procured from generators, including reserve used to deal with variability of wind and contingency management, and PFR scheduled for post-fault frequency security.

5.4. Modelling Transmission Network Constraints

To illustrate GB power system operation practices, transmission network constraints have been introduced in the COEF model via DC optimal power flow, which can optimise the provision of energy and frequency regulation services, while managing transmission network congestion cost effectively. Furthermore, for security concerns, preventive control for management of network congestions has been incorporated into the COEF model, which is modelled as a certain percentage of line capacity reductions. In this context, the GB power system shall be capable of experiencing an outage of a single transmission circuits without causing losses in the electricity supply. In response to this, the COEF software tool is extended to include consideration of contingencies (modelled as line capacity reduction) and determining preventive control actions while minimising the total system operation costs.

As illustrated in Figure 5.6, the simplified GB power system [10], including 13 buses and 19 transmission links, is used for the following case studies, where 592 generators with a capacity value and the UC parameters have been integrated. Interconnectors (i.e., NEMO (To Belgium), ElecLink (To France), IFA (To France), IFA2 (To France), Britned (To Netherlands), NSL (To Norway), Moyle (To Ireland), EWIC (To Ireland), Viking (To Denmark)) with changing import and export limits have been integrated into the co-optimisation model, which may influence the largest loss of generation and demand. To mimic realistic GB operation practices, RESs are mainly located at the north of the UK (e.g., Scotland), while conventional generators (e.g., gas-fired power plants) are allocated at the south of the UK (e.g., England). Since the simplified GB network has 18 transmission lines, 19 scenarios are considered, including the base scenario (without contingencies) and 18 outage scenarios, where each outage scenario involve one different transmission line with a certain percentage of line capacity reduction.

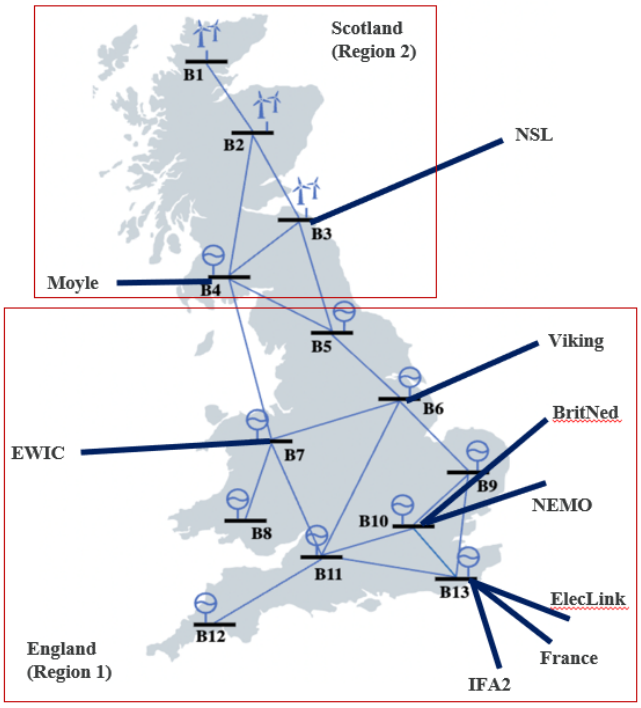

Figure 5.6: Illustration of the simplified GB power network utilised in updated software tool, where 'B' refers to 'bus' and the navy blue lines represent interconnectors.

To demonstrate the influence of line capacity reduction on the optimisation results, a detailed comparison among 5 different cases has been conducted, including: 1) without contingencies, available network capacity (while taking into account contingencies) is 2) 60% 3) 50% 4) 40% and 5) 30%. The daily operation cost associated with these different cases are presented in Figure 5.7.

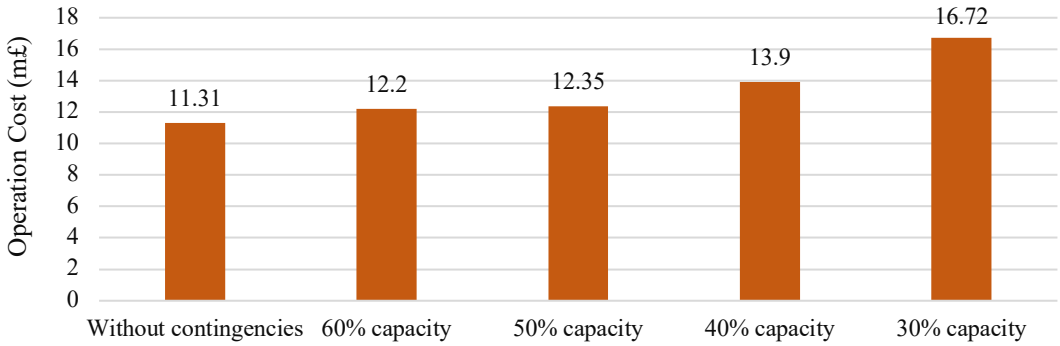

Figure 5.7: Comparison of daily operation cost and computing time under 5 different cases, considering different level of network capacity under contingencies

It can be observed from Figure 5.7 that reducing the line capacity from 100% to 30% will increase the operation costs, because of the necessity to part-load conventional generators for preventive control. It is notable that this case study is based on one selected operating day, while the results of operation costs may significantly change

under different system conditions (e.g., different demand level and/or wind generation etc.)

5.5. Influence of Adding Frequency-related Constraints

Furthermore, since the focus is to investigate the influence of frequency-related constraints (e.g., frequency Nadir, RoCoF, and q-s-s) on the co-optimisation results, it will be necessary to analyse the addition of frequency-related constraints on the operation costs under the above 5 cases presented in the previous section. As illustrated in Figure 5.8, including frequency-related constraints accounting for both under and over frequency requirements can significantly increase the daily operation costs, due to the increase in the number of part-loaded generators for inertia provision.

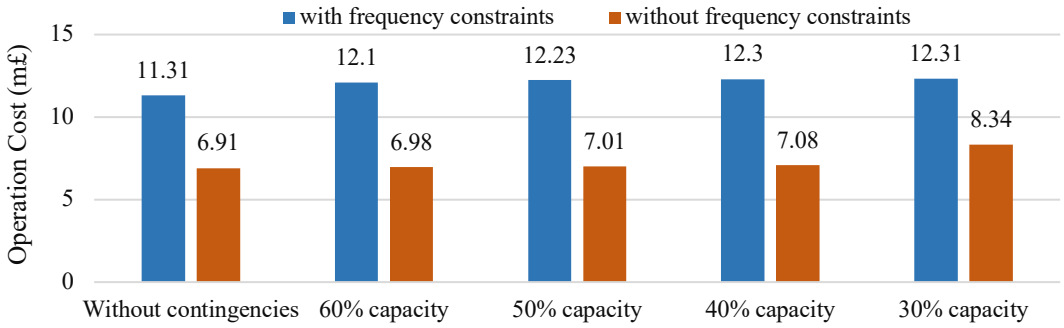

Figure 5.8: Comparison of operation cost under two scenarios: a) with frequency constraints, b) without frequency constraints

5.6. Synthetic Inertia and Demand-side Inertia

The provision of extra inertia from auxiliary sources (e.g., thermal generators, rotating loads, or even wind generators) could support frequency control. Thermal generators and rotating loads could be manufactured with a higher inertia constant, while wind generators could potentially provide "synthetic inertia" through a supplementary control loop in the wind turbine controller. An increased system inertia would induce a decrease in operational costs, as it would not be necessary to schedule as many thermal plants to comply with dynamic frequency regulation. As it can be seen in Figure 5.9, the value of inertia increases significantly with the installed capacity of wind generation.

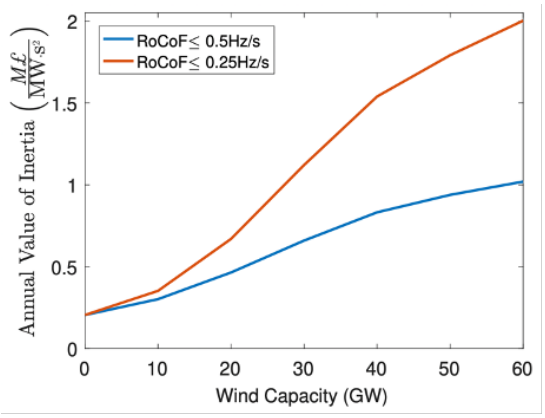

Figure 5.9: Annual value of inertia for different levels of wind capacity

This figure also shows that relaxing the RoCoF requirement to 0.5Hz/s would reduce the value of inertia (and corresponding ancillary services costs). Nevertheless, inertia would still have a significant value in this scenario.

As indicated in Figure 5.10, the main difference between synchronous inertia and synthetic inertia from wind is that the latter has a 'recovery effect' [11]: as the wind turbine decelerates to provide synthetic inertia, it deviates from the Maximum-Power-Point Tracking (MPPT), therefore the power delivered to the grid by the turbine in the 'post-inertial' period is lower than the power in the 'pre-fault' period.

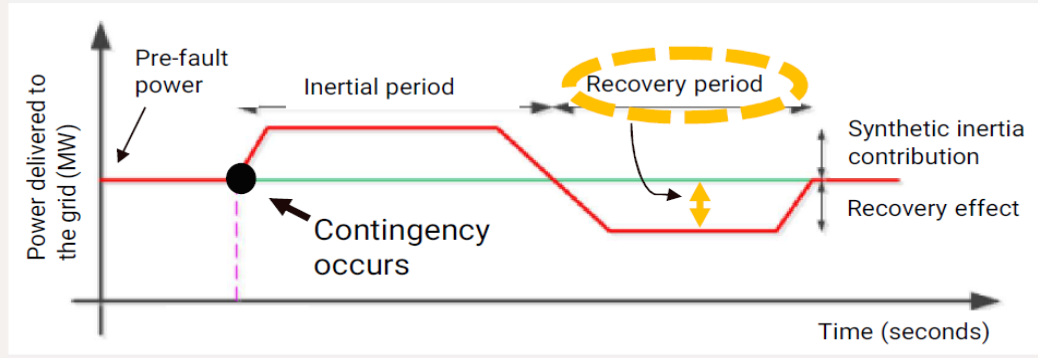

Source: NERC Industry Webinar, White Paper: Fast Frequency Response Concepts and Bulk Power System Reliability Needs

Figure 5.10: Illustration of synthetic inertia from wind turbines and the recovery effect

Two main categories of grid-connected inverters have been defined, depending on their controls: grid-following (GFL) and grid-forming (GFM) technologies. GFM inverters are growing on the agenda as these would allow the grid to operate without synchronous machines [12]. In this context, the developed software tool has been extended to consider the synthetic inertia from wind turbines, while the recovery effects have been precisely modelled.

To demonstrate the benefits of frequency services from wind turbines, a comparison case study has been carried out, including two cases: a) Case 1: Wind turbines do not provide frequency response services; b) Case 2: 30% of wind turbines are equipped with GFM inverters and therefore have the capability to provide synthetic inertia. The rest of wind turbines can provide enhanced frequency response. The operation costs under these two case studies are presented in Figure 5.11, where different RoCoF limits (e.g., 0.125 Hz/s, 0.5 Hz/s, and 1 Hz/s) have been considered for a more comprehensive comparison. It can be found that the daily operation cost can be reduced significantly under different RoCoF limits, when wind turbines can provide frequency response services (i.e., synthetic inertia and enhanced frequency response). As illustrated in Figure 5.12, when wind frequency services are considered, the number of part-loaded generators is reduced, which can lead to lower thermal generation level and then lower operation costs and carbon emission. It is also notable that, in the case of limited

synthetic inertia capability from wind turbines, there may be benefits from equipping batteries with synchronous condensers for inertia provision.

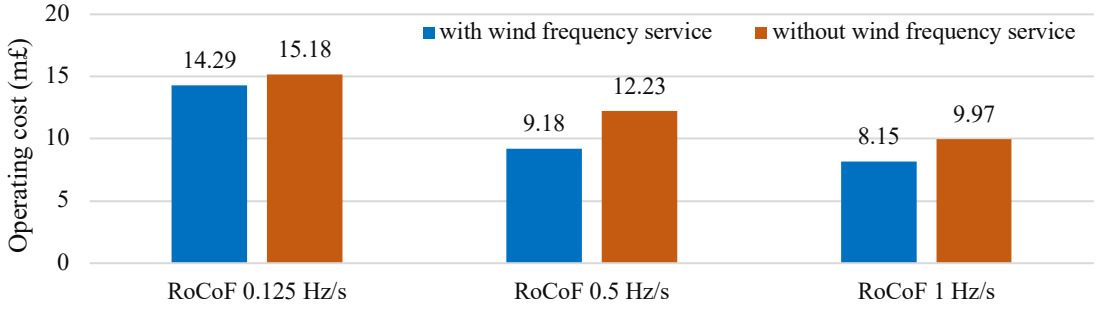

Figure 5.11: Daily operation cost comparison under two different cases: a) wind turbines do not provide frequency response services; b) 30% of wind turbines are equipped with GFM inverters and therefore have the capability to provide synthetic inertia

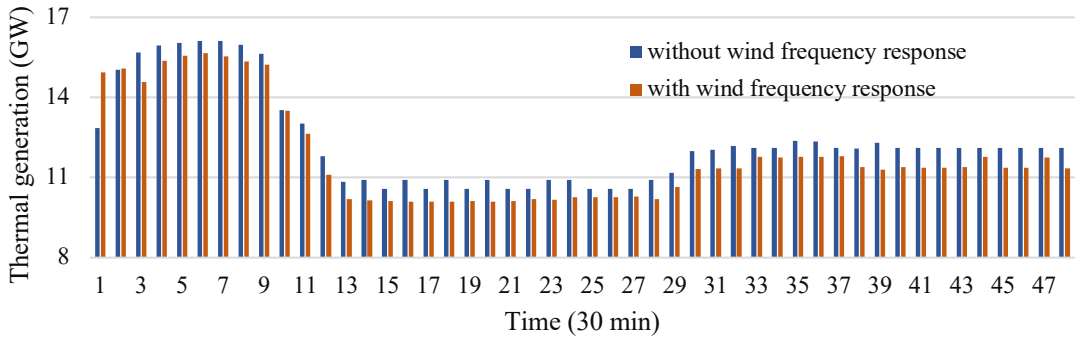

Figure 5.12: Commitment of thermal generation under two different cases: a) wind turbines do not provide frequency response services; b) 30% of wind turbines are equipped with GFM inverters and therefore have the capability to provide synthetic inertia

Except for inertia provision from the generation side, the modelling of demand-side inertia has also been incorporated into the developed software tool. Even though there have been studies estimating that 35% of demand would provide inertia on average, it is notable that variable frequency drives are expected to be more widely deployed in the demand side, which would in turn reduce inertia from demand [8]. As a result, this report assumes that 5%-10% demand can provide inertia with a 5 s inertia constant [8]. As illustrated in Figure 5.13, considering demand-side inertia can significantly reduce the daily operation costs and may also sightly increase the system inertia level depending on certain data inputs.

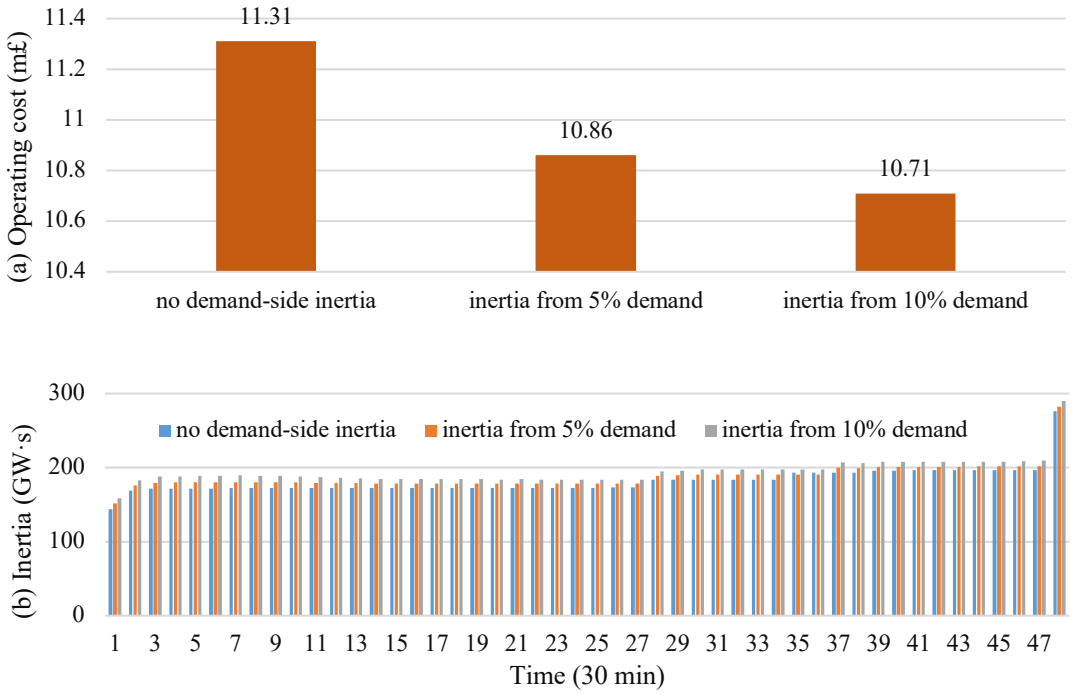

Figure 5.13: Illustration of the influence of demand-side inertia on a) operation costs and b) overall system inertia level

5.7. The Choice of 'Optimised Largest Loss'

One solution for the low-inertia challenge consists of reducing the largest possible outage in the system. In the GB system, this would be achieved by part-loading interconnectors under certain system's conditions, as these are the largest sources of power in the grid. In this context, the largest loss is considered as a decision variable in the UC, which then optimises the system's operation by dynamically balancing the cost of de-loading and the savings from a reduced need for inertia and frequency regulation services (PFR, DC). Decreasing the largest loss might be optimal depending on the demand and RES-based level of generation in the system. As depicted in Figure 5.14, reducing the largest loss could have a significant positive impact on the cost of frequency services, particularly for future scenarios with high wind penetration.

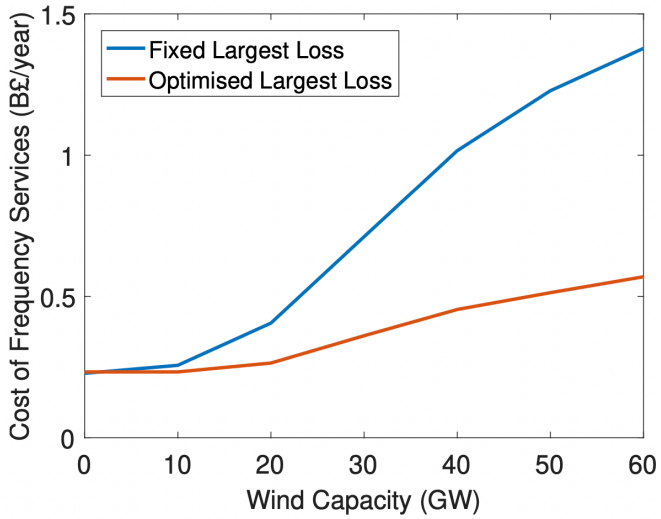

Figure 5.14: Annual cost of frequency services under different wind-penetration scenarios, for the largest possible loss of 1.32GW.

In order to analyse the influence of including optimised largest loss, a comparison case study has been conducted, including two cases: a) case 1: the energy price is 47 £/MWh, the price for an interconnector or a nuclear plant is 10 £/MWh. The DC price is 10 £/MWh; b) case 2: the energy price is 20 £/MWh, the price for an interconnector or a nuclear plant is 10 £/MWh. The DC price is 10 £/MWh. In this analysis, the range of the largest loss that may be from the interconnector or nuclear plant is between 1.62 GW and 1.8 GW. Note that any other resources that may cause the largest loss can also be deployed. It can be observed from Figure 5.15 that the model will not choose to reduce the largest loss, when the price difference between the energy price and the interconnector/nuclear power plant is bigger than the DC price. On the other hand, the model will choose to reduce the largest loss, when the price difference between the energy price and the interconnector/nuclear power plant is equal to or smaller than the DC price.

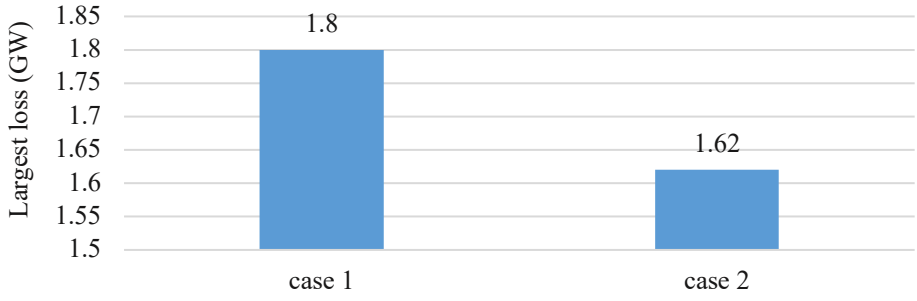

Figure 5.15: The largest losses under two different cases

Furthermore, a more detailed sensitivity Analysis on the influence of DC price on the choice of ‘reducing largest loss’ is conducted, where we assume that the energy price is

47 £/MWh and the price for the interconnector or nuclear plant is 10 £/MWh. As depicted in Figure 5.16, the model does not choose to reduce the largest loss, when the DC price is lower than the price difference 37 £/MWh. However, when the DC price is higher than 37 £/MWh, the model decides to reduce the largest loss. Note that '1' in Figure 5.20 means 'the model decides to reduce the largest loss', while '0' means 'the model doesn't choose to reduce the largest loss'.

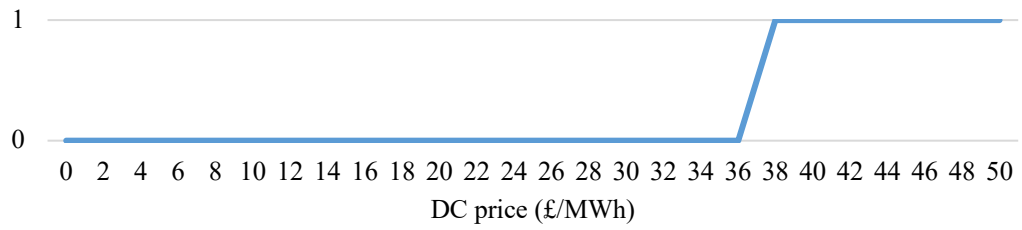

Figure 5.16: Influence of DC price on the choice of 'reducing largest loss or not'

5.8. Securing both Regions under Regional Frequency Model

The case studies above analyse the implications of securing against the largest loss in England (region 1). However, since the system operator needs to maintain stability in the entire GB, the system scheduling must actually be secured for the outages in either region: the contingencies of the largest loss in both England and Scotland should be considered. To clearly demonstrate this point, a detailed comparison analysis has been conducted, including three cases: a) only securing region 1 (England); b) only securing region 2 (Scotland); c) securing both regions simultaneously.

As presented in Figure 5.17, there cases are considered: 'only securing region 1', securing region 2' and 'securing both regions' showing that the low inertia level in Scotland may significantly increase the GB operation costs. Furthermore, the case 'securing both regions' receives slightly higher daily operation costs than the case 'securing region 2', because of the strict requirements for securing both regions, i.e., accounting for the potential largest loss in both England and Scotland.

Figure 5.17: Operation cost comparison under three cases: a) secure region 1, b) secure region 2, c) secure both regions

6. Summary of the Testing and Results

6.1. Test Result Summary

The following key requirements from National Grid ESO have been tested:

- **Model validation:** Compare the metered post fault frequency profile of actual events with the simulated post fault frequency profile of the MATLAB simulation tool, using a time resolution of 1 second. With each model, record the simulated frequency profile (e.g. f-sim) and the difference between the simulated and actual frequency data as the model's accuracy (±f-acc) for each second to give an accuracy profile for the particular event.
- **Dynamic Frequency Requirements:** The constraints associated with Rate-of-Change-of-Frequency (RoCoF), Nadir, and quasi-steady-state requirements are included in the model, which determines the dynamic frequency control requirements.
- **Co-optimisation of DC with Inertia and PFR:** The software tool co-optimises energy delivery and provision of all frequency regulation services and system inertia at minimum whole-system costs, while maintaining energy balance and frequency stability.

In summary, COEF models have been successfully run using the 16-day data provided, and all results have been recorded and uploaded to the SharePoint. Models provide correct results related to frequency services (PFR, DC, and inertia) to meet frequency security requirements. Three-day results have been tested via the dynamic simulation tool.

6.1.1. Comparison between MATLAB and real-world frequency curves

National Grid has kindly provided 16 days of events with real-world frequency evolution data for us to test our MATLAB Tool, where the basic assumptions of the simulation tool are listed below:

- Inertia, PFR, DC and the largest loss are used as the input data.
- PFR and DC are assumed to ramp up from zero at the first second, where the delivery speeds of PFR and DC are 10 seconds and 1 second, respectively.
- Dealing with the potential largest loss, while meeting RoCoF and Nadir constraints, is the main scope of this project.
- Frequency RoCoF, Nadir and Q-S-S are key constraints for frequency security.

Specifically, the following events have been highlighted for testing:

- 18/04/2022 17:25, '*Generator Trip, with a loss of 1200MW. Nothing further to add.*'

Input data: 1) Inertia 211 GWs, 2) PFR 0.411 GW, 3) DC 0.653 GW, and 4) Generation loss 1.2 GW, where DC has been doubled to consider potential enhanced frequency

response (EFR). Potential firm frequency response (FFR) that may have an influence on frequency evolution (e.g., 'static' and 'dynamic primary') has been included in PFR.

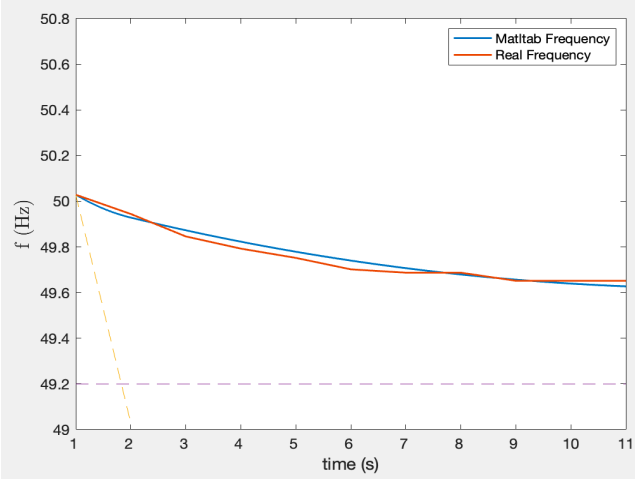

Figure 6.1: Test results of the event on 18/04/2022 17:25

The largest frequency deviation occurs in the 10th second with the value of 0.035 Hz, while the minimum frequency deviation is 0 Hz. In summary, the average frequency deviation is around 0.018 Hz. To summarise, it can be found that the curves are basically the same, verifying the reliability of the MATLAB dynamic simulation tool.

- 21/04/2022 05:09, '*Demand Trip, with a loss of 500MW whilst exporting., Nothing further to add.*'

Input data: 1) Inertia 181.1 GWs, 2) PFR 0.14 GW, 3) DC 0.316 GW, and 4) Demand loss 0.5 GW.

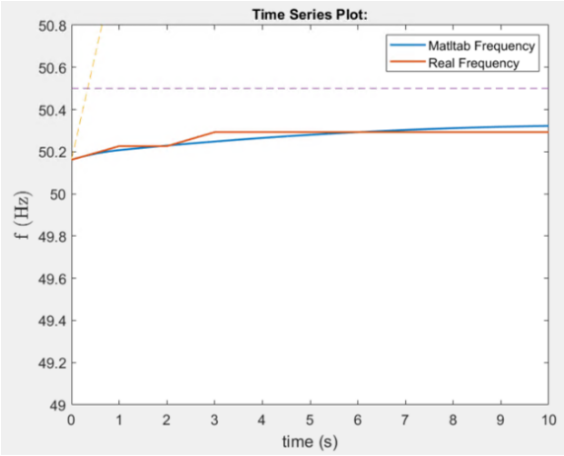

Figure 6.2: Test results of the event on 21/04/2022 05:09

In this case, both curves show similar trend (it is not clear why there are frequency increases at 3rd second) – according to the data, the balance between demand and

supply is not changed (no further demand loss). In summary, the curve from MATLAB tool demonstrates that the RoCoF is the same. The MATLAB tool exhibits smaller frequency deviations, compared with the real frequency curve. The largest frequency difference is around 0.05 Hz at the 3th second, while the smallest frequency difference is 0 Hz. The average frequency difference is around 0.017 Hz.

- 04/11/2023 5:54, '*Similar incidents to those described on this list, Cascade tripping of 3 units from a single generator: At 05:57:32 a unit trips with a loss of approx 465MW, At 05:57:39 a second unit trips with a loss of approx 465MW, At 05:58:56 a third unit trips with a loss of approx 605MW.*'

Input data: 1) Inertia 141.3 GW, 2) PFR 0.117 GW, 3) DC 0.47 GW, 4) Generation Loss 0.465 GW, and 5) After 8 sec, another 0.465 GW loss happens.

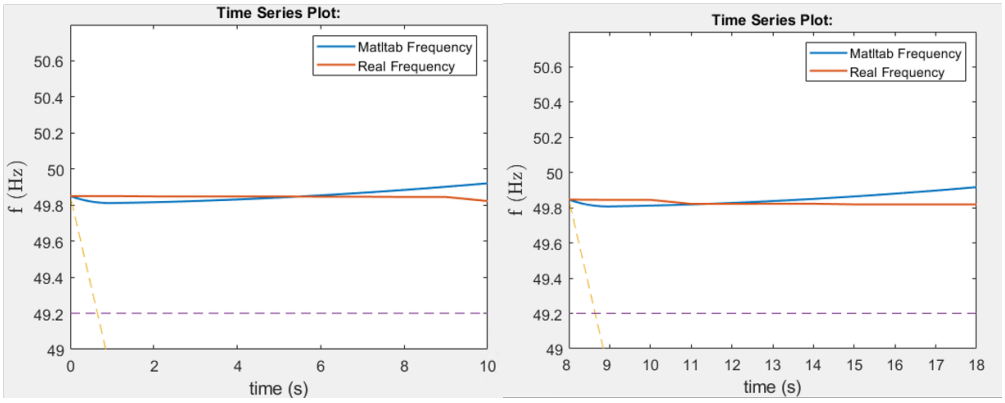

Figure 6.3: Test results of the event on 21/04/2022 05:57

In general, the MATLAB frequency curve and real-world frequency curve look like very similar. The curve from MATLAB tool exhibits smaller frequency deviations. The largest frequency difference is around 0.1 Hz at the 10th second, while the smallest frequency difference is 0 Hz. The average frequency difference is around 0.022 Hz.

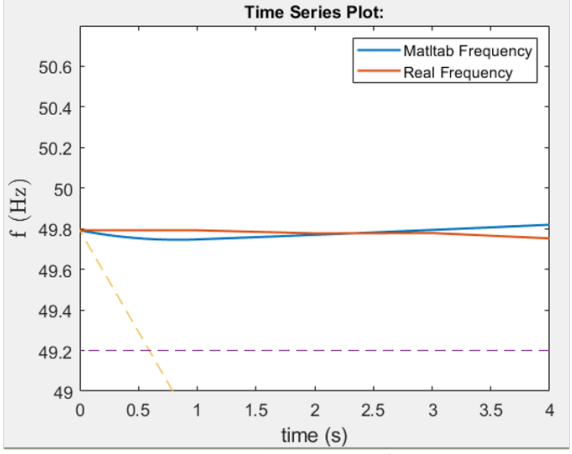

Figure 6.4: Test results of the event on 21/04/2022 05:58

Similarly, the MATLAB frequency curve and real-world frequency curve look like very similar under the event on 21/04/2022 05:58. The largest frequency difference is around 0.08 Hz at the 4th second after the loss, while the smallest frequency difference is 0 Hz. The average frequency difference is around 0.02 Hz.

- 22/12/2023 13:06, Similar incidents to those described on this list, Bipole tripped at 13:10 with a loss of 1000MW instantaneously.

Input data: 1) Inertia 125 GW, 2) PFR 0.098 GW, 3) DC 0.872 GW, and 4) Generation Loss 1 GW.

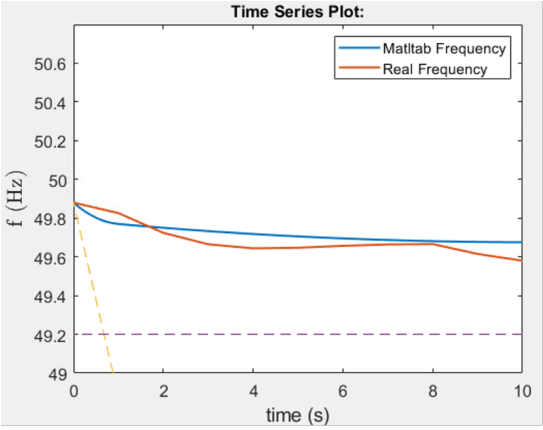

Figure 6.5: Test results of the event on 22/12/2023 13:06

In general, the MATLAB frequency curve and real-world frequency curve look like very similar. The curve from MATLAB tool exhibits smaller frequency deviations. The largest frequency difference is around 0.08 Hz at the 4th second, while the smallest frequency difference is 0 Hz. The average frequency difference is around 0.048 Hz.

To summarise, the figures from approximate MATLAB tool do show a very similar trend with the true frequency curves (although these are not exactly the same) – specifically, RoCoF and frequency Nadir are very similar across the case performed.

Potential reasons for the differences of frequency curves are also summarised below:

- This project scope is focused on the co-optimisation of PFR, DC, inertia and optimised loss to meet the frequency security constraints (RoCoF, Nadir, Q-S-S) at minimum costs. For some events, we doubled the DC quantity and the RoCoF and Nadir constraints are met. Data for some other frequency services (e.g., EFR) is not available.
- The accuracy of provided data may also influence the dynamic simulation results, e.g., the accurate quantity of the loss, the accurate occurring time point, potential data collection delays, etc.
- In the approximate MATLAB tool (and the detailed COEF model), it is assumed that PFR is fully delivered in 10 seconds and DC is fully delivered in 1 second,

with constant ramping rates, as presented in slide 2 (given the guidance provided at the beginning pf the project). On the other hand, these services may be delivered in different times.

- Secondary Frequency Response is not considered as it does not begin delivery until 30 seconds after the event, which is outside the scope of the model.

6.1.2. Demonstration of Co-optimisation results

In order to clearly demonstrate the superior performance of the enhanced software tool in achieving the co-optimisation of energy and frequency services towards regional frequency security, extensive case studies have been carried out, using 16 days of data provided by National Grid ESO. As illustrated in Figure 5.8, the simplified GB power system [10], including 13 buses and 18 transmission links, is used for the following case studies.

Specifically, the input demand and wind profiles in day 1 have been illustrated in Figure 6.6, while the co-optimisation results of frequency ancillary services are demonstrated in Figure 6.7. It can be found that PFR and DC have been procured to maintain frequency security, showing a certain level of complementary effect. Additionally, the inertia provision results meet the minimum inertia requirement (140 GWs), while the potential largest loss is around 2 GW in day 1. After obtaining the co-optimisation results, we have done frequency tests via the MATLAB dynamic simulation tool, where the test results are depicted in Figure 6.8. It can be observed that the schedules of frequency services (inertia, PFR, and DC) can always maintain frequency security, e.g., RoCoF and frequency Nadir constraints.

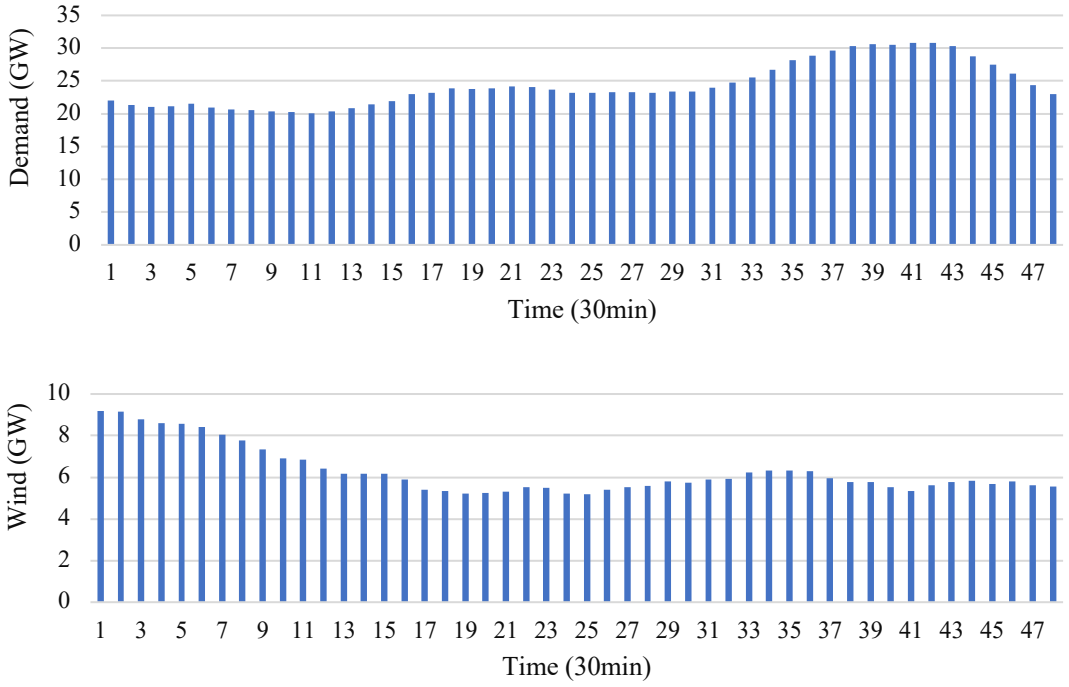

Figure 6.6: Demand and wind profiles in day 1

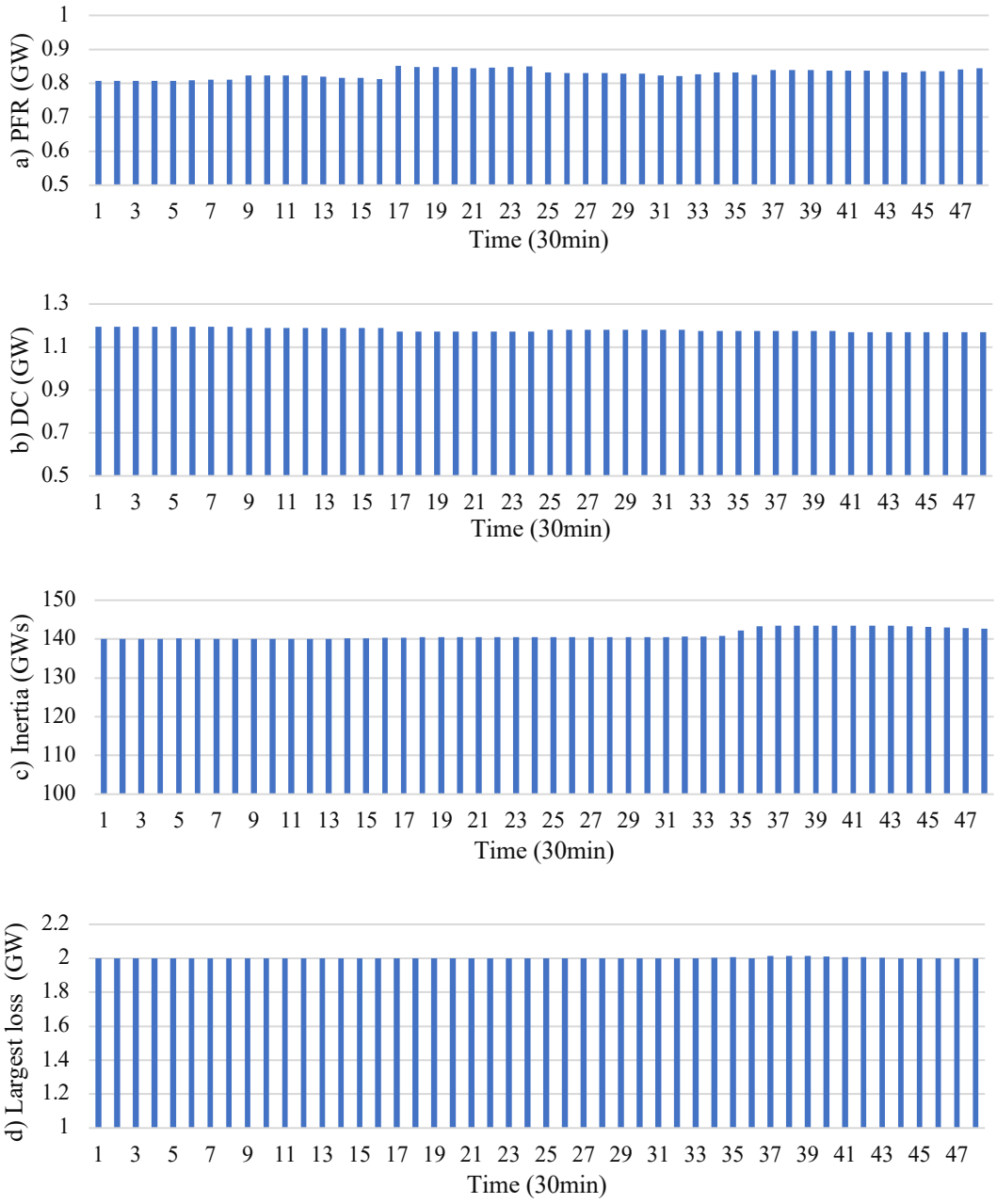

Figure 6.7: Scheduling results of frequency services: a) PFR, b) DC, c) inertia, and d) optimised largest loss

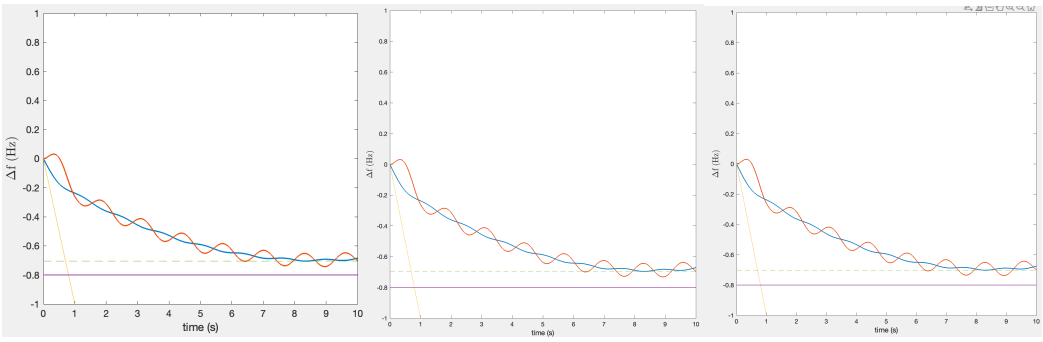

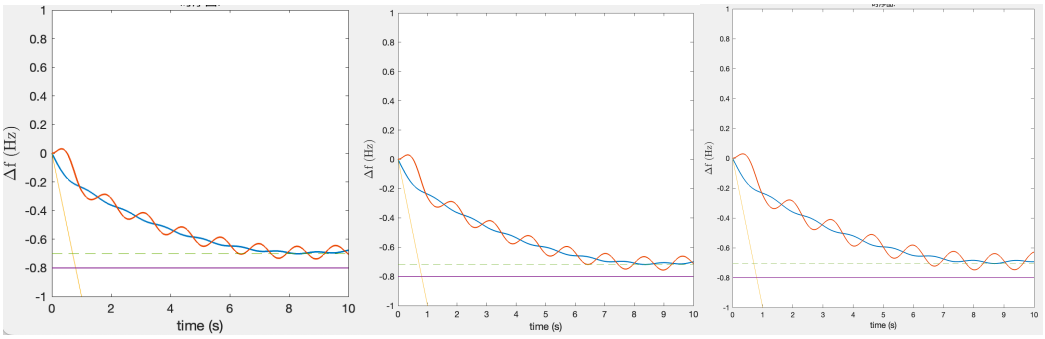

Figure 6.8 Test results of the MATLAB dynamic simulation tool: a) time step 0, b) time step 8, c) time step 16, d) time step 24, e) time step 32, f) time step 40

To summarise, it can be concluded that the COEF model has successfully co-optimised energy and various frequency services, achieving minimum operation costs while maintain frequency security. We have tested all 16 days of data using the COEF model, where all the scheduling results and MATLAB test results have been submitted to National Grid ESO.

6.2. Sensitivity Analysis

To further verify the accuracy of the COEF model, we have conducted a detailed sensitivity analysis by changing the values of different input parameters (e.g., uniform or regional frequency models, RoCoF limits, demand-side inertia levels, wind synthetic inertia levels and minimum inertia levels), where the results are illustrated in Figures 6.9-6.13.

Figure 6.9 demonstrates that considering frequency constraints can lead to increased operation costs (18.9%), due to the extra procurement of various frequency ancillary services (e.g., PFR and DC) and the requirement of minimum inertia level (140 GWs) for system security. In addition, regional frequency model obtains slightly higher daily operation costs (2.4%) than uniform frequency model, due to the consideration of regional frequency oscillations and extra needs for ancillary services. Figure 6.10 illustrates that relaxing RoCoF limits can lead to significant cost savings. For example, relaxing RoCoF limit from 0.125 Hz/s to 1 Hz/s brings 41.8% reduction of daily operation costs.

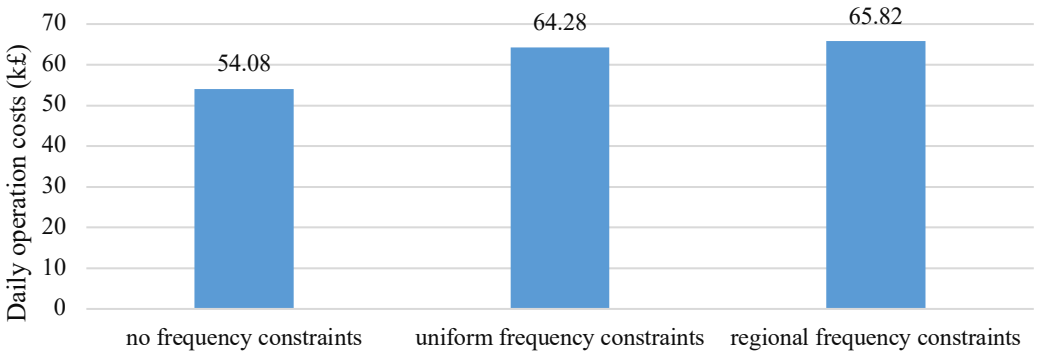

Figure 6.9 Cost comparison of three types of models: a) economic operation model without

frequency constraints, b) uniform frequency model, c) regional frequency model

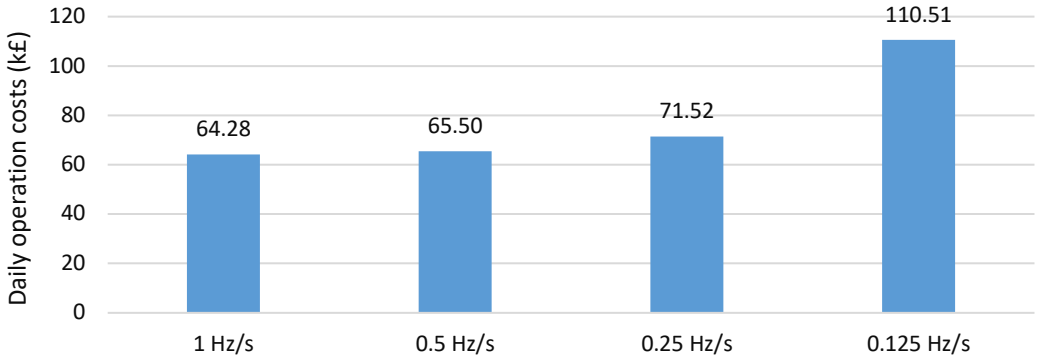

Figure 6.10 Sensitivity analysis on the influence of RoCoF limits on daily operation costs

Figures 6.11 and 6.12 depict the influence of demand-side inertia level and wind synthetic inertia level on daily operation costs, respectively. In general, increasing demand-side inertia level from 5% (i.e., 5% demand can provide inertia) to 20% can obtain 2.3% reduction of operation costs. Similarly, increasing the percentage of wind generation for synthetic inertia from 0% to 20% can obtain 1.8% reduction of operation costs.

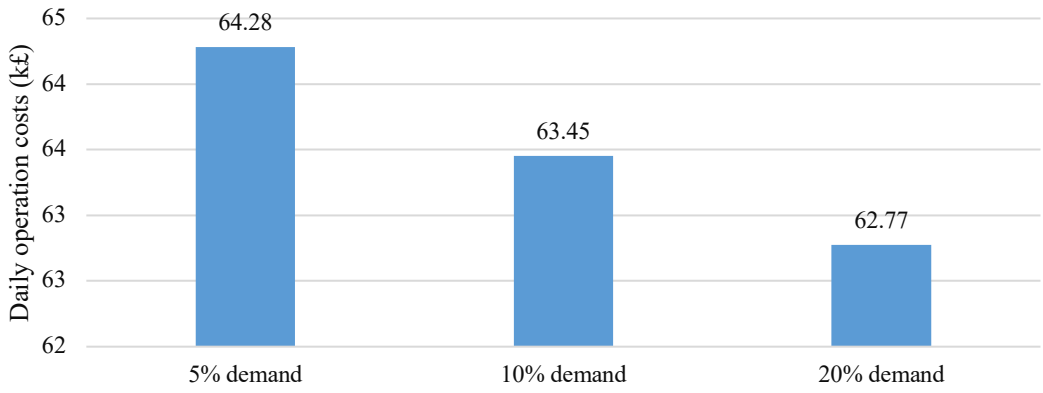

Figure 6.11 Sensitivity analysis on the influence of demand-side inertia level on daily operation costs

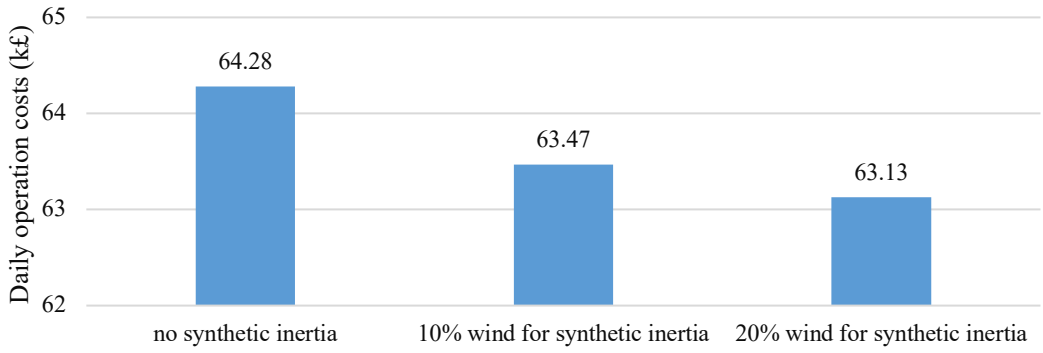

Figure 6.12 Sensitivity analysis on the influence of wind synthetic inertia level on daily operation costs

Finally, the influence of 'minimum inertia level' is depicted in Figure 6.13. It can be observed that relaxing the minimum inertia level from 140 GWs to 100 GWs can bring visible cost savings (7.2% reduction of daily operation costs).

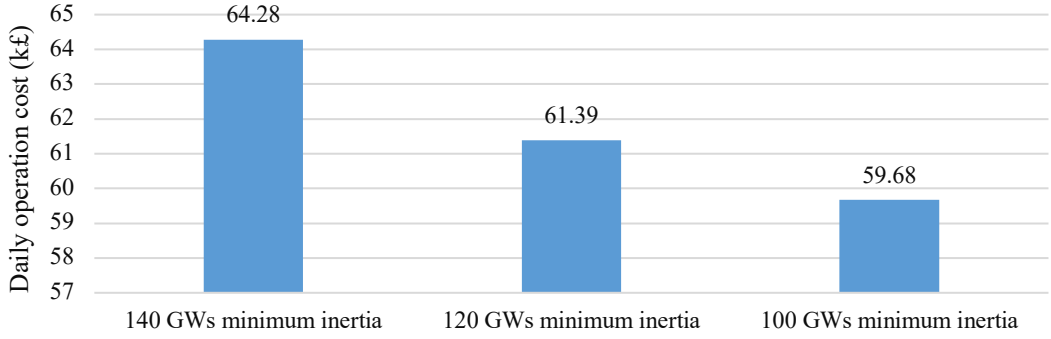

Figure 6.13 Sensitivity analysis on the influence of minimum inertia level on daily operation costs

7. Current Operational Practices in the Control Room

According to the Grid Code [6], data for any Operational Day may be submitted to The Company up to several days in advance of the day to which it applies, as provided in the Data Validation, Consistency and Defaulting Rules. However, Interconnector Users must submit Physical Notifications, and any associated data as necessary, each day by 11:00 hours in respect of the next following Operational Day in order that the information used in relation to the capability of the respective External Interconnection is expressly provided. Based on the above information, almost all the input data will be sent to ESO at least one-day ahead, which will not influence the scheduling of the COEF model.

According to the Grid Code [14], the data may be modified by further data submissions at any time prior to Gate Closure, in accordance with the other provisions of BC1. The data to be used by The Company for operational planning will be determined from the most recent data that has been received by The Company by 11:00 hours on the day before the Operational Day to which the data applies, or from the data that has been defaulted at 11:00 hours on that day in accordance with BC1.4.5. Any subsequent revisions received by The Company under the Grid Code will also be utilised by The Company. In the case of all data items listed below, with the exception of item (e), Dynamic Parameters (Day Ahead), the latest submitted or defaulted data, as modified by any subsequent revisions, will be carried forward into operational timescales. Based on the above information, it is also possible to run the COEF model every hour or even every half-an-hour for the next 24 hours, in order to consider the latest data submissions prior to Gate Closure.

To summarise, the COEF model currently operates at day ahead, therefore integrating the tool with the control room systems only affects the ANSE (Assistant National Scheduling Engineer, 24 hours to 8 hours ahead of real time) and NSE (National Scheduling Engineer, 8 hours to 4 hours ahead of real time) roles, and all their associated day-ahead policies, processes and procedures. The ANSE role only performs the day-ahead assessments once a day (7 days a week) on morning shifts. Other teams outside the control room that operate from 1 year down to 2 days ahead of real time will be unaffected by the COEF model, as the model only applies to day-ahead timescales, however it may give the added benefit of offsetting the costs of other contracts procured at day ahead and helping with profiling requirements for dynamic containment.

Considering the difference between COEF model and current operational practice, it might be necessary to integrate the tool into a new system, which can be performed by Control Engineers. Since the tool is very straightforward, it can be anticipated that running the tool will not influence the quality of work produced by the Control Engineer. In general, the COEF model is only used once a day, taking around 25-30 minutes to obtain co-optimisation results of energy, reserve and frequency services (inertia, PFR, and DC); thus, it may take around one hour for the Control Engineer to run the model and then collect results.

8. Needs and Requirements for the Evolution of the Prototype

The current COEF model is run in a day-ahead fashion with a half-an-hour resolution. However, in current ESO operational practices, the ESO still takes balancing actions from gate closure, 89 minutes ahead of real time down to real time. Thus, it is possible to further modify the tool to allow it to be run every hour or every half-an-hour for the next 24 hours, after receiving all the necessary input data. Considering the high complexity of current model (e.g., detailed UC setup for around 600 generators, consideration of preventive control, reserve, etc.), it may be necessary to simplify certain embedded functions to speed up the model solving procedure, e.g., reducing the number of generators, simplifying the UC setup, etc., which can shorten model solving time and allow it to be run every hour or every half-an-hour.

The developed COEF model is equipped with the function of ‘reserve modelling’ including both ‘up reserve’ for generation drop and ‘down reserve’ for demand reduction, which can be used to balance the risk of uncertainty at day-ahead. Additionally, as aforementioned, the model can be potentially run every hour or every half-an-hour rather than only ‘day-ahead’, which can also mitigate the influence of uncertainties.

To fully integrate the tool into the ESO Control Room, it is very necessary to conduct system tests and system integration tests.

9. Conclusions

Imperial College has developed a novel software tool that can achieve cost-effective co-optimisation of energy and frequency services. The software tool can conduct day-ahead UC schedules with half-an-hour resolution. Various frequency services including inertia, PFR, DC, and reduced largest loss have been included in the co-optimisation model. In detail, the inertia provision can be from conventional generators, converter-interfaced resources (e.g., wind turbines), and demand side, while DM and DR have been incorporated into the software tool as input parameters that might influence DC procurement. In addition, the software tool has been extended to include network constraints, reserve requirements, and both over and under frequency security requirements, where contingencies are modelled as a certain percentage of line capacity reduction. Furthermore, the model has been extended to consider the regional frequency-related constraints in a two-region power system, including frequency Nadir, RoCoF and Q-S-S. The software tool includes two types of operation modes, i.e., centralised optimisation for the minimisation of overall operation costs and 'self-dispatching' optimisation for the minimisation of 'self-dispatching' costs. A simplified GB power system integrated with around 600 generators has been employed as the platform to test the proposed frequency-secured framework, demonstrating that it is a key to procure inertia and frequency response appropriately among the different regions of the system (e.g., England and Scotland).

Finally, detailed test results of the key functions in the COEF model has been provided in this report, including the model validation by comparing real-world and MATLAB frequency curves and result validation by using 16 days of data to test the COEF model. Overall, the figures from approximate MATLAB tool do show a very similar trend with the real frequency curves, including both RoCoF and frequency Nadir, even though they are not exactly the same. The potential reasons leading to these small differences could be unknown quantity of other frequency services (e.g., EFR), data accuracy (e.g., accurate quantity of the loss and accurate event occurring time), simplified MATLAB tool settings (e.g., constant ramping rate assumption), etc. In general, we consider these small differences are acceptable. Furthermore, given the 16-day scheduling results of frequency services (inertia, PFR, and DC), we can conclude that the COEF model can successfully co-optimise energy and frequency services, achieving minimum costs while maintaining frequency security.

References

[1] F. Teng, V. Trovato, and G. Strbac, “Stochastic scheduling with inertia-dependent fast frequency response requirements,” IEEE Transactions on Power Systems, vol. 31, no. 2, pp. 1557–1566, 2016.

[2] “Frequency risk and control report,” UK National Grid ESO, Report, 2022. [Online]. Available: https://www.nationalgrideso.com/document/248151/download.

[3] “Assessment of risks resulting from the adjustment of RoCoF based loss of mains protection settings,” Energy Networks Association, Report, 2015. [Online]. Available: https://www.nationalgrid.com/sites/default/files/documents/Appendix%201%20Strathclyde%20Report%201.pdf

[4] L. Badesa, F. Teng, and G. Strbac, “Simultaneous scheduling of multiple frequency services in stochastic unit commitment,” IEEE Transactions on Power Systems, vol. 34, no. 5, pp. 3858-3868, 2019.

[5] X. Zhang, G. Strbac, N. Shah, F. Teng, and D. Pudjianto, “Whole-system assessment of the benefits of integrated electricity and heat system,” IEEE Transactions on Power Systems, vol. 10, no. 1, pp. 1132–1145, 2018.

[6] “Electricity System Operator Markets Roadmap,” UK National Grid ESO, Report, 2023. [Online]. Available: https://www.nationalgrideso.com/document/278301/download.

[7] “New Dynamic Services (DC/DM/DR),” UK National Grid ESO, Report, 2022. [Online]. Available: https://www.nationalgrideso.com/document/276606/download.

[8] L. Badesa "Towards a cost-effective operation of low-inertia power systems." (2020).

[9] “Short Term Operating Reserve Assessment Principles,” UK National Grid ESO, Report, 2021. [Online]. Available: https://www.nationalgrideso.com/document/222391/download.

[10] “Carbon intensity API - national data,” UK National Grid ESO, 2021. [Online]. Available: https://carbonintensity.org.uk/.

[11] J. Ekanayake and N. Jenkins, “Comparison of the response of doubly fed and fixed-speed induction generator wind turbines to changes in network frequency,” IEEE Transactions on Energy Conversion, vol. 19, no. 4, pp. 800–802, 2004.

[12] L. Badesa, C. Matamala, Y. Zhou, and G. Strbac, "Assigning Shadow Prices to Synthetic Inertia and Frequency Response Reserves from Renewable Energy Sources," IEEE Transactions on Sustainable Energy, vol. 14, no. 1, pp. 12-26, 2022.

[13] L. Badesa, F. Teng, and G. Strbac, "Conditions for regional frequency stability in power system scheduling—Part II: Application to unit commitment," IEEE Transactions on Power Systems, vol. 36, no. 6, pp. 5567-5577, 2021.

[14] The Grid Code | ESO. [Online]. Available: https://dcm.nationalgrideso.com/